1972

# Grain Sorghum Canopy Temperature as a Function of Meteorological Conditions

Charles Gregg Carlson

# GRAIN SORGHUM CANOPY TEMPERATURE AS A FUNCTION OF METEOROLOGICAL CONDITIONS

BY

CHARLES GREGG CARLSON

A thesis submitted
in partial fulfillment of the requirements for the
degree Master of Science, Major in
Agronomy, South Dakota
State University

1972

GRAIN SORGHUM CANOPY TEMPERATURE AS A FUNCTION

OF METEOROLOGICAL CONDITIONS

This thesis is approved as a creditable and independent investigation by a candidate for the degree, Master of Science, and is acceptable for meeting the thesis requirements for this degree. Acceptance of this thesis does not imply that the conclusions reached by the candidate are necessarily the conclusions of the major department.

Thesis Adviser Date

Head, Plant Science Department Date

# ACKNOWLEDGMENTS

The funds for this research were provided by South Dakota State University Agricultural Experiment Station and instrumentation by the South Dakota Water Resources Institute.

I wish to express my gratitude to Dr. Maurice L. Horton, Associate Professor of Plant Sciences, for his advice, assistance and encouragement which made this work and its completion possible.

Appreciation is extended to Hal Werner, Assistant Hydrologist of the Remote Sensing Institute and to the Remote Sensing Institute for providing the photographs for this paper. To Loyd Stone, Graduate Assistant, for his stimulating conversation which resulted in some of the conclusions of this paper. I am grateful to Debbie Tarkelson for her help in the data processing and to John DeWitt for his help in the drawing of figures.

CGC

# TABLE OF CONTENTS

# LIST OF FIGURES

FIGURE PAGE

# INTRODUCTION

Research in the physics of evaporation and transpiration has been the subject of interest to a large number of scientists, but especially to those of us concerned with the frequent drought problems in the Great Plains Region. Within the last few years the fallacious idea that water is an inexhaustible free commodity has been disspelled and replaced by the realization that good water is an important natural resource that must be properly managed and conserved in order to assure adequate amounts in the future.

About 70% of the water that falls on the Continental United States is utilized, not as most of us would expect, by drainage into our vast rivers and lakes, but by direct evaporation from our soil surface or by transpiration from plants. It is estimated that three thousand billion gallons of water per day are returned to the atmosphere from the soil and plants in the United States (Conaway and Van Bavel, 1967).

As weather modification and water management become more practical in the Great Plains Region, it is going to be more and more important and necessary for us to be able to predict rapidly and accurately the water, nutritional, and thermal properties of soil and plants.

Presently the only feasible methods for determining the physical conditions of soils and plants require ground truth observations. Determining the conditions over a large area is difficult if not impossible without large numbers of people and equipment utilizing much time and expense.

With recent developments and improvements in aircraft and satellite capabilities, it is now possible to view remote sensing imagery taken from many different spectral passbands, representing large land areas. In order for imagery to be of practial importance, adequate information for analyzing and interpreting the imagery is necessary. During the growing season radiation in the infrared spectrum does not penetrate deeply into a crop canopy, therefore, imagery in this spectral passband is imagery of the crop canopy. To properly interpret canopy imagery, knowledge of the interaction between the crop and its environment must be known. I assert that the status of crop transpiration rate and viability, which are closely associated with soil water, nutrition, and meteorological conditions, can be determined as a function of the deviation of the crop canopy temperature from the ambient air temperature.

In order to determine the manner in which the crop canopy temperature responds to meteorological conditions, a study was initiated with the following objectives:

1. Evaluate the departure of surface temperature from ambient temperature for various soil, plant, and weather conditions.
2. Test the applications of surface temperature-evapotranspiration equations against other well-known evapotranspiration equations.
3. Develop a reliable evapotranspiration equation based on the temperature of the evaporating surface.

# LITERATURE REVIEW

For many years the study of evaporation from the soil surface and transpiration through the plant canopy has been the subject of interest to researchers concerned with moisture utilization and conservation, and several equations purporting to predict evapotranspiration have been developed. These equations can be classified into five types, each representing a different approach. A brief description of each type will follow.

The first type equation is based upon mass transport of heat and water. Dalton's type equation can be expressed as follows (Slatyer et. al., 1970)

$$ET = f((ESC - EB), WSPD) \qquad (1)$$

where

ET = evapotranspiration (gm cal $cm^{-2}$ $min^{-1}$ $gm^{-1}$)

ESC = saturation vapor pressure at the surface (mb)

EB = actual vapor pressure at height ZB above the surface (mb)

WSPD = wind speed function.

The second type of equation is the Aerodynamic approach. The basis for the aerodynamic method is the idea that the flux of heat and water vapor operate by similar mechanisms of transfer. The following two equations express this idea:

$$FLH = -(DEAIR)(SPHT)(KH)\frac{dT}{dZ} \qquad (2)$$

where

FLH = flux of sensible heat

DEAIR = density of air (gm / $cm^3$)

SPHT = specific heat of air (cal $gm^{-1}\,{}^{o}C^{-1}$)

KH = eddy diffusivity or transfer coefficient for heat

$\frac{dT}{dZ}$ = partial of temperature with respect to height.

$$FLW = -(DEAIR)(KV)\frac{dq}{dZ} \qquad (3)$$

where

FLW = flux of water vapor

KV = eddy diffusivity or transfer coefficient for water vapor

$\frac{dq}{dZ}$ = partial of specific humidity with respect to height.

The third type is the Energy Budget method. This method is based on the equation:

$$RNET = RSOL - ROUT = SFLX + AELX + M + ET + P \qquad (4)$$

where

RNET = net radiation (all units gm cal $cm^{-2}$ $min^{-1}$ $gm^{-1}$)

RSOL = incoming radiation

ROUT = outgoing radiation

SFLX = soil heat flux

AFLX = air heat flux

M = miscellaneous term

ET = evapotranspiration

P = photosynthesis.

Since P and M terms are usually less than the experimental error obtained in the measurement of the other major parameters, they can be left out without any serious error (Rosenberg et. al., 1968). This gives

$$RNET = SFLX + AFLX + ET. \quad (5)$$

Bowen (1926) postulated that the heat flux into the soil was absorbing only a small fraction of the net radiation. He combined this idea with the aerodynamic approach to give:

$$ET = FLW = -(DEAIR)(KV)(L)(WMOL)\frac{de}{dZ} \quad (6)$$

where

L = latent heat of vaporization (cal $gm^{-1}\,^{o}C^{-1}$)

PR = atmospheric pressure (mb)

$\frac{de}{dZ}$ = partial vapor pressure with respect to height.

This equation differs from equation (3) in that it uses vapor pressure rather than specific humidity.

$$AFLX = FLH = -(DEAIR)(SPHT)(KH)\frac{dT}{dZ} \quad (7)$$

$$B = \frac{AFLX}{ET} = \frac{FLH}{FLW} = \frac{(PR)(SPHT)\ (T)}{(L)\ (WMOL)\ (q)} \quad (8)$$

where

B = Bowen ratio

T = temperature gradient

q = vapor pressure gradient.

Combining equations (8) and (6) we get

$$ET = \frac{RNET - SFLX}{1 + B} \quad (9)$$

The fourth type is the bookkeeping method. This method takes the form of a balance sheet. Total water into the system is determined by addition of precipitation and irrigation. Total water out of the system is determined by the addition of surface runoff, tile drainage and ET. Deep percolation has usually been assumed to be negligible, but recent studies have indicated that this assumption may be erroneous

(LaRue et. al., 1968).

The fifth type to be considered is the combination of two or more of the first four methods. The objective of the combination method is to utilize the most valuable parts of other methods in order to obtain an improved equation. Two of the combination equations that I consider of importance are Van Bavel's Equation and Bartholic's Equation. Van Bavel (1966) combined surface energy balance, water vapor transfer and sensible heat transfer from the aerodynamic approach to obtain the following:

$$ETVB = \frac{(SEVT)(HENG) + (LA)(TFC)(EVAD)}{SEBT + 1} \qquad (10)$$

where

ETVB = potential evapotranspiration by Van Bavel (gm cal $cm^{-2}$ $min^{-1}$ $gm^{-1}$)

SEVT = slope of the saturation vapor pressure curve (mb/°C) divided by the psychrometric constant (0.65 mb/°C)

HENG = the sum of the energy imputs exclusive of sensible heat and evapotranspiration (gm cal $cm^{-2}$ $min^{-1}$ $gm^{-1}$)

LA = latent heat of vaporization constant (586 cal/gm)

TFC = turbulent transfer coefficient that accounts for wind in the equation (gm $cm^{-2}$ $min^{-1}$ $mb^{-1}$)

EVAD = saturation vapor pressure deficit of the atmosphere above the crop surface (mb).

Bartholic (1970) derived a combination equation for potential evapotranspiration using essentially an energy balance approach and a modified Bowen ratio in which the actual surface temperature was used.

$$ETBA = \frac{RFRI + SFLX}{(TDBB - TSF)/(ESB - ESC)} \quad (11)$$

where

ETBA = potential evapotranspiration by Bartholic (gm cal $cm^{-2}$ $min^{-1}$ $gm^{-1}$)

RFRI = net radiation from Fritschen net radiometer (gm cal $cm^{-2}$ $min^{-1}$ $gm^{-1}$)

SFLX = soil heat flux (gm cal $cm^{-2}$ $min^{-1}$ $gm^{-1}$)

TDBB = temperature dry bulb above the surface ($^{o}C$)

TSF = surface temperature ($^{o}C$)

ESB = saturation vapor pressure at temperature TDBA (mb)

ESC = saturation vapor pressure at temperature TSF (mb).

In evapotranspiration research in recent years, a great amount of work has been done estimating evapotranspiration for specific small microclimates. The idea of point evapotranspiration has overshadowed the concept of regional evapotranspiration. Morton (1969) developed an interesting regional potential evapotranspiration concept. He states that many conditions are the result of the dynamic moisture supply within a region as opposed to moisture conditions of a region being the result of the atmospheric climatology. This argument relating cause and effect may sound trival and would probably be considered a waste of time but for the consequences that this reversal of thinking brings out. It leads to a very healthy and important contribution to the definition of potential evapotranspiration.

Morton (1969) defines potential evaporation as evaporation from a continuously moist surface which is subjected to regional radiation

absorption, vapor transfer, and heat transfer characteristics. It comprises an area so small that the transfer of heat and water vapor have no significant effect on the evaporability of the overpassing air.

This definition is in disagreement with the idea that potential evaporation is evaporation that would occur from a continuously moist infinite surface. Based on this idea, the evaporability of the air would decrease as the air passes over the surface and the air's vapor pressure is increased. This idea is further complicated in that potential evaporation is usually measured with a lysimeter, which is far too small to meet the specifications of the definition.

In evapotranspiration research the plant is the principal vehicle for the transpiration of water. I assert that insufficient attention is given to the plant by scientists working on the physical aspects of evapotranspiration and even less attention is given to the physical environment by scientists working on the physiological aspects.

It is a fairly well understood principle that plant roots rarely meet the transpirational demand upon the plant during periods of the day with high incoming energy. However, they usually recover fully at night (Gardner, 1960). This becomes much more significant when we realize that a plant may transpire two to five times its own water holding capacity in a single day (Millington, 1970). The plant-soil system is a dynamic system which seldom reaches a stable equilibrium. The soil is a moisture sink and the plant acts as a pump attempting to drain the sink in response to atmospheric demand.

Water moves from the plant roots to the transpiring leaves along pressure gradients which are referred to as gradients of diffusion

deficit. With an increase in evaporative demand, there is also a rise in the diffusion pressure deficit which causes a decrease in turgor pressure but an increase in water absorption pressure at the root. The decrease in turgor pressure is evident by a decrease in leaf water potential. These pressure decreases result in a decrease in the permeability of the plant to water flow. Consequently, there is a reduction in the rate of transpiration (Denmead et. al., 1962).

Monteith (1965) discussed the effect of different weather parameters upon the evapotranspiration of a crop surface. He stated that, assuming leaf resistance to water flow remains constant, evaporation increases (1) linearly with radiation, (2) linearly with saturation vapor pressure (3) with temperature, if radiation and saturation vapor pressure deficit remain constant (along the slope of the saturation vapor pressure curve implied but not actually stated), and (4) with convective forces as a function of changes in surface temperature and rate of exchange. If the heat supply is positive, an increase in wind speed decreases leaf temperature. Cooling of the leaf tends to decrease losses of sensible and latent heat but this effect is compensated for by an increase in the rate of exchange. When the rate of exchange more than compensates for the decrease in temperature, the loss of sensible heat is increased at the expense of latent heat and transpiration rates decrease with an increase in wind speed

Denmead and Shaw (1962) reported that under conditions of a high atmospheric potential evapotranspiration rate, the actual transpiration rate may be well below the potential rate even if the soil water content is above what is considered to be an ample supply. Under periods of low

potential evapotranspiration, the actual evapotranspiration may equal the potential evapotranspiration rate even though soil moisture is limiting.

Idso et. al. (1966) reported that different plant species vary greatly in their reflecting and absorbing properties. Not only are the spectral properties of the canopy of various crops different, but the stage of growth for many species has a great deal of influence on how their spectral properties behave. For example, an increase in the rate of chlorophyll development has been related to a decrease in reflective properties.

One of the major limiting factors in the study of the physical aspects of evapotranspiration has been the inability to make an accurate measurement of the actual canopy temperature of the crop being studied. Recent availability of the radiation thermometer has made possible accurate determinations of canopy temperatures. By using a bandpass outside the principal water vapor and carbon dioxide emission bands, it is possible to view a selected surface area and to determine its temperature remotely and accurately. Figure 2.1 shows emissive properties of air at different wave bands.

The determination of temperature is based upon the Stephan-Boltzmann electromagnetic radiation equation that will be discussed later.

Fuchs and Tanner (1966) and Conaway and Van Bavel (1967) have indicated that accuracies of $\pm$ 0.2$^{o}$C may be obtained if the emittance of the surface under study is known.

There has been controversy over the accuracy obtained if the emissivity of the plant is assumed to be one. There have been arguments

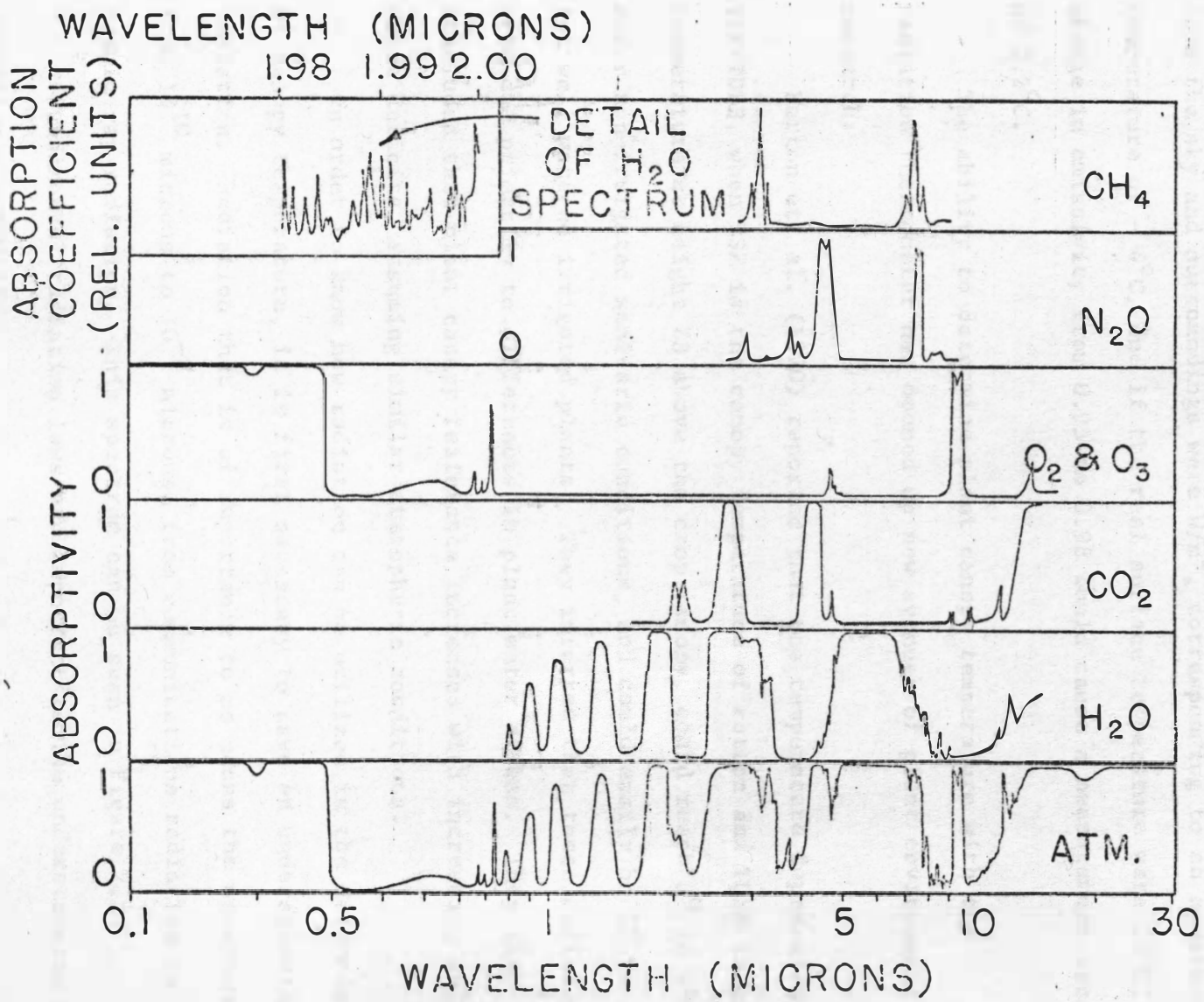


Figure 2.1. Absorption spectra for $H_2O$, $CO_2$, $O_2$, $N_2O$, $Ch_4$, and the atmosphere from Fleagle et. al. (1963).

by Monteith and Szeicz (1962), and Gates (1963) that the error due to not correcting for emissivities would only amount to 0.2°C. However, Fuchs and Tanner (1966) have pointed out that if the thermal radiation from the sky and surroundings were W/$m^2$, corresponding to an apparent temperature of - 4°C, and if the real surface temperature were 25°C, the change in emissivity from 0.95 to 0.98 would cause a measurement error of 2.2°C.

The ability to determine plant canopy temperature with the radiation thermometer has opened up new avenues of plant environment research.

Horton et. al. (1970) reported that the temperature depression, TSF-TDBB, when TSF is the canopy temperature of cotton and TDBB is air temperature at height ZB above the crop canopy, could reach 3° to 4°C under non-irrigated semi-arid conditions, and could easily be 1° to 2°C for well watered irrigated plants. They inferred that these differences were due primarily to differences in plant water stress. They also concluded that plant canopy resistance increases with increasing soil water deficits, assuming similar atmospheric conditions.

In order to know how radiation can be utilized in the determination of canopy temperature, it is first necessary to have an understanding of radiation. Radiation that is of importance to us scans the spectrum of from $10^{10}$ microns to $10^{-8}$ microns, from communications radiation to cosmic ray radiation. This spectrum can be seen in Figure 2.2.

Fundamental radiation laws are important to the understanding of radiation thermometry.

Some of the basic units and conversions of radiation physics used

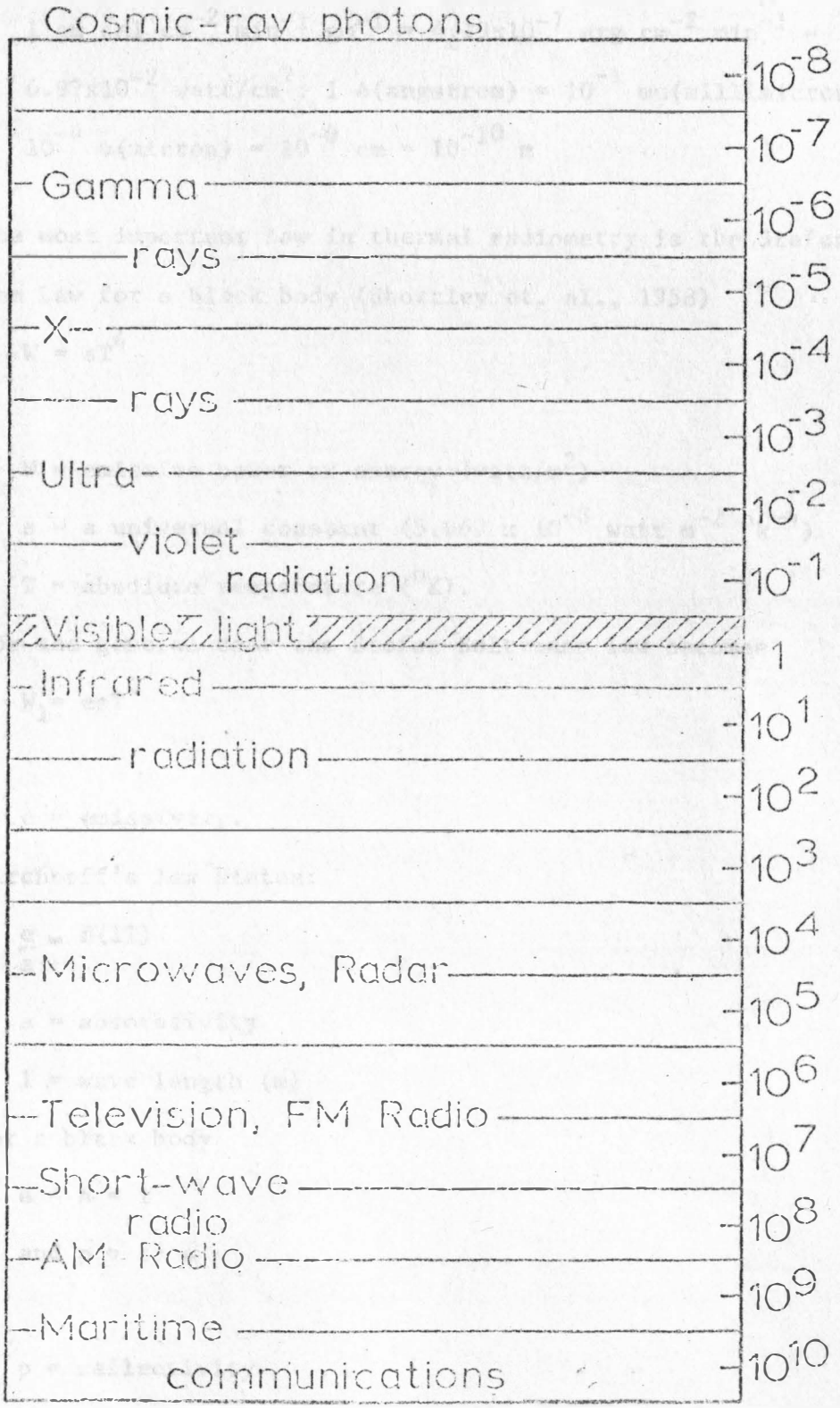


Figure 2.2. Radiation spectrum from $10^{10}$ microns to $10^{-8}$ microns.

in this paper are:

$1\ gm\ cal\ cm^{-2}\ min^{-1}\ gm^{-1} = 4.19 \times 10^{-7}\ erg\ cm^{-2}\ min^{-1} = 6.97 \times 10^{-2}\ watt/cm^2$: 1 A(angstrom) = $10^{-1}$ mu(millimicron) = $10^{-4}$ u(micron) = $10^{-8}$ cm = $10^{-10}$ m

The most important law in thermal radiometry is the Stefan-Boltzmann Law for a black body (Shortley et. al., 1958)

$$W = sT^4 \tag{12}$$

where

W = emissive power or energy ($watt/m^2$)

s = a universal constant ($5.669 \times 10^{-8}$ watt $m^{-2}\ {}^{o}k^{-4}$)

T = absolute temperature ($^{o}K$).

For the general case the Stefan-Boltzmann law becomes

$$W_1 = esT^4 \tag{13}$$

where

e = emissivity.

Kirchhoff's law states:

$$\frac{e}{a} = f(1T) \tag{14}$$

a = absorbtivity

1 = wave length (m)

For a black body

$$e = a = 1 \tag{15}$$

$$\text{and } p = t = o \tag{16}$$

where

p = reflectivity

t = transmittance.

The next important equation is Planck's Equation for the shape of the wavelength versus energy curve

$$W_1 = \frac{2n(10^{-9})(h)(c^2)}{1^5(\exp[(h)(c)/(1)(K)(T)]-1)} \qquad (17)$$

where

$W_1$ = energy in Watt $m^{-2}$ $mu^{-1}$

C = speed of light (2.99793 x $10^8$ m/sec)

K = Boltzman's constant (1.3804 x $10^{-23}$ joule / $^oK$)

h = Planck's constant (6.625 x $10^{-34}$ joule sec).

From Planck's displacement law we see that f(lT) vanishes as l approaches o and when l = 0.

Wien's Displacement Law is essential in the determination of maximum emittance as a function of wave length (Sulton, 1953)

$$l_{max}\ T = 2940 \qquad (18)$$

where

$l_{max}$ = maximum energy wave length of emittance at temperature T.

From this equation we can determine the wave length at which the maximum energy intensity can be found. From Figure 2.3, which is a graphic representation of Planck's black body function for the sun's absolute temperature and the earth's absolute temperature, we can see that the sun emits its maximum energy intensity at about 0.5u and almost all of the radiation from the sun falls between 0.15u and 4.0u. The earth, with a temperature of about 300$^oK$, has its maximum intensity emitting wave length at about 10u with practical limits of output between 3u and 80u.

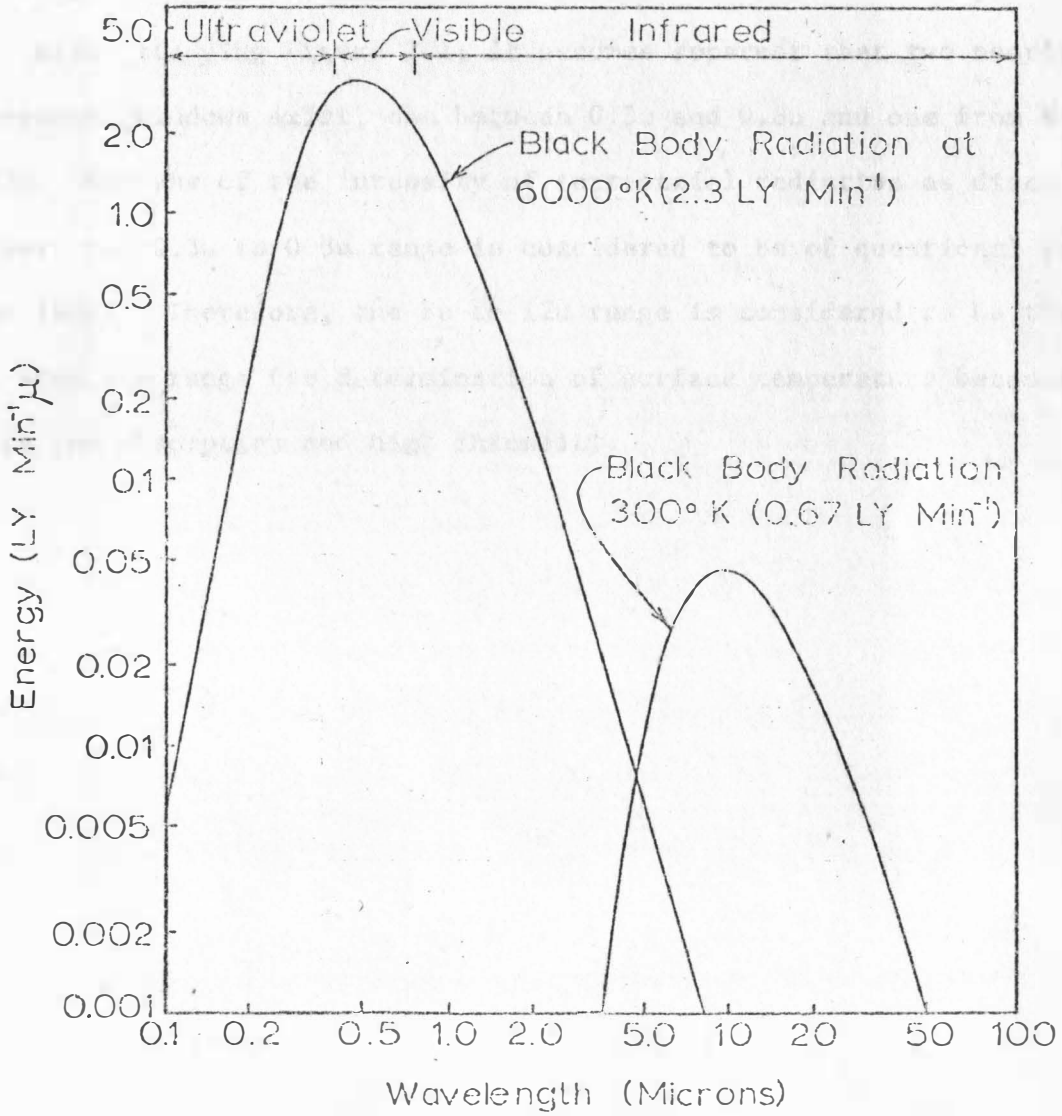


Figure 2.3. Black body spectra of solar and terrestrial radiation.

As mentioned earlier, Figure 2.1 shows absorption properties of different wavelength bands of radiation. In order to be able to measure absolute temperatures using the Stephan-Boltzmann Equation we must find a "window" in the atmosphere. A window is defined as a range of wave length in which little radiation is absorbed by the atmosphere.

After studying Figure 2.1, it becomes apparent that two nearly transparent windows exist, one between 0.3u and 0.8u and one from 8u to 12u. Because of the intensity of terrestrial radiation as discussed earlier, the 0.3u to 0.8u range is considered to be of questional value (Rose 1969). Therefore, the 8u to 12u range is considered to be the most accurate range for determination of surface temperature because of its low absorption and high intensity.

# INSTRUMENTATION, MATERIALS AND METHODS

## Canopy Temperature

Canopy temperature was determined with a Barnes Infrared Thermometer (radiometer) Model IT-3. The Barnes radiometer is functional for determination of temperatures from -45°C. to 204 °C. It measures the spectral passband from 8 to 14 microns.

The Barnes radiometer was mounted on a trolley as shown in Figure 3.2 and 3.3, which was positioned 3 meters above the ground surface. The trolley traversed a span of 7 meters in a time period of 13.5 minutes, which is a speed of 0.52 meters per minute. Styrofoam insulation was placed over the signal preamplifier and the sensing head in order to insure that no error was obtained from instrument heating as discussed by Jackson and Idso (1969). Calibration was obtained by using an aluminum plate painted with Parsons Black paint, and embedded thermocouples. The plate was placed at a height of one meter above the soil surface and located over a sorghum row. In this manner, it served as a point for calibration and for reference. Plate temperatures were recorded every ten minutes throughout the duration of the experiment, thus insuring accuracy of the Barnes radiometer and its proper calibration. The calibration curve can be found in Figure 3.4.

Emissivites were determined with a black box as has been described by Buettner and Kein (1965). The box used in this study is shown in Figure 3.5. The box used was square with an open bottom. The four vertical interior sides were covered with mirrors. The top consisted of two layers. The first layer was 0.64 cm aluminum plate painted on

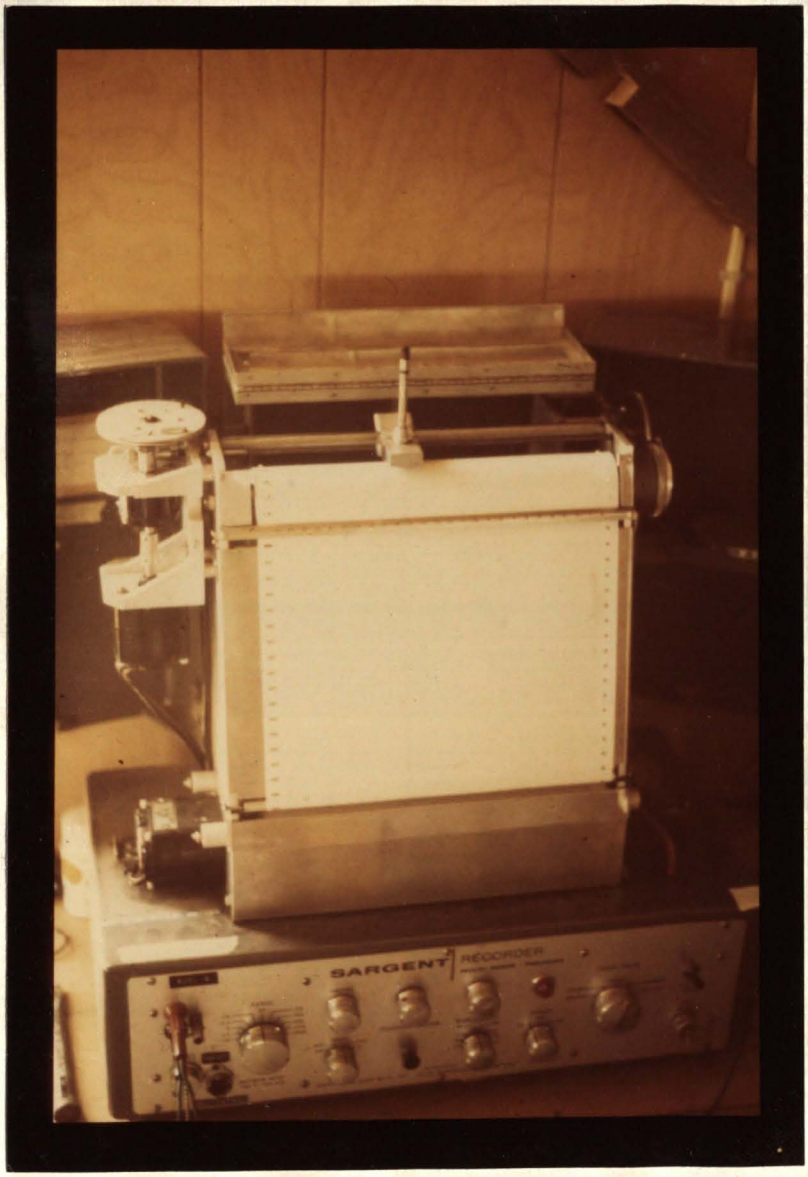


Figure 3.1. Sargent recorder model MR.

Figure 3.2. Barnes radiometer, scanner and blackbody calibrator.

Figure 3.3. Barnes radiometer and scanner in operation.

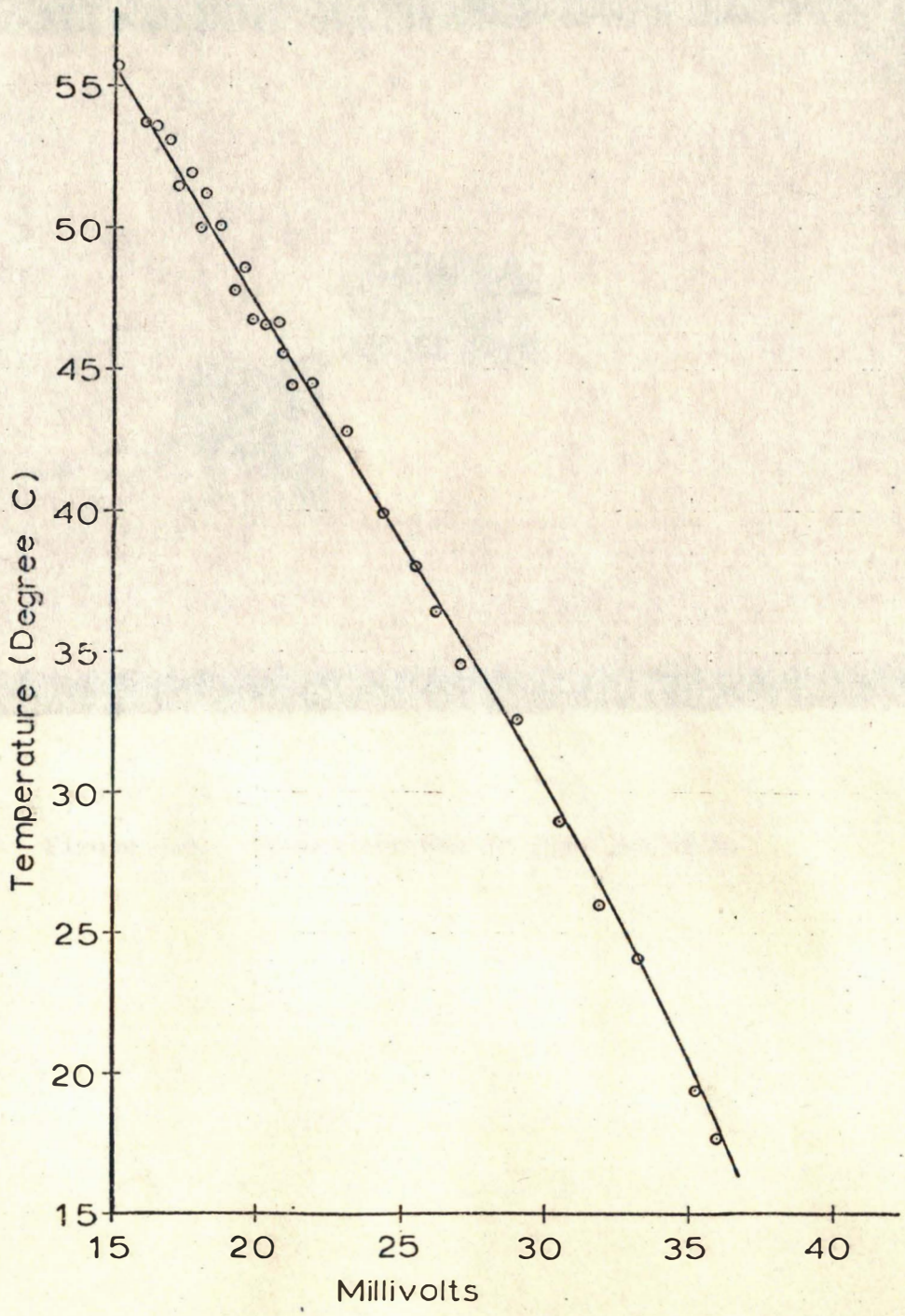


Figure 3.4. Calibration regression curve for Barnes radiometer.

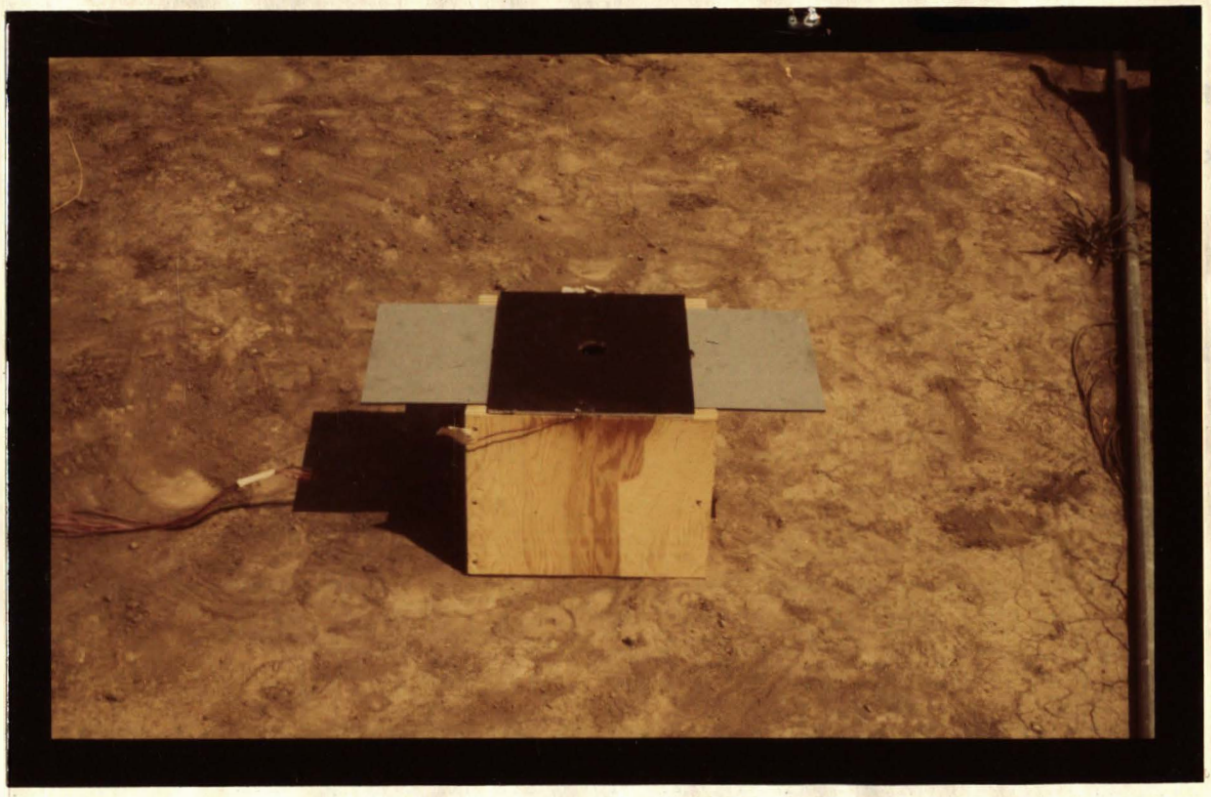

Figure 3.5. Emissivity box in open position.

top and bottom with Parsons Black paint. Embedded into the aluminum plate were two thermocouples. In the middle of the plate there was a hole large enough to accommodate the Barnes radiometer head. The layer beneath the aluminum plate consisted of two mirrors, each covering half of the box. There was a semicircle cut into the side of each mirror so that when they were joined in the middle they formed a hole the same size as the hole in the aluminum plate. When the top mirrors were pulled out as they are in Figure 3.5, the surface viewed by the radiometer was similar to the view as seen without the box. When the mirrors were pushed in, the chamber was essentially a perfect reflector and the radiometer viewed the surface as a black body. Calculated emissivites for the calibrator plate and the plant canopy were found to be within .01 of each other. Therefore, the calibration regression was already correcting for emissivites.

Humidity

The humidity data used in this thesis has not been recorded as humidity data in tabular form, but has been used in the various equations for the determination of evapotranspiration in which humidity parameters are required.

Humidity was determined with Honeywell SSP129 Dew Probe sensors. The dew probe is an electrically heated self regulating dew point hygrometer. It consists of two wire electrodes wound around a cloth sleeve which is impregnated with lithium chloride. The lithium chloride absorbs moisture causing the impregnated cloth to become a conductor

which results in electrode heating. This causes evaporation until an equilibrium point is obtained. The equilibrium temperature is monitored by means of a thermocouple inside the cloth sleeve. This temperature is porportional to the dew point temperature. Aspiration over the probe was provided in order to assure proper sampling. Humidity equipment was calibrated with two Bendix mercury thermometer wet and dry bulb psychrometers.

Radiation

Short wave or solar radiation from the sun has a predominant wavelength from 0.3 to 3 microns. Roughly half of this radiation falls within the visible spectrum, 0.4 to 0.7 microns. This is distinguished from emitted long wave radiation which is greater than 3 microns in wavelength (Rose, 1960). Solar radiation was determined with an Eppley 180° pyrheliometer. It consists of thermal junctions placed in two rings. The inner ring is blackened with Parsons Black and the outer ring is smoked with white magnesium oxide. These two surfaces provide a temperature difference which generates an output proportional to the incident radiation. A hermetically sealed glass bulb limits the response to the wavelengths greater than 0.3 and less than 3.5 microns.

Outgoing radiation was measured with a Kipp Model G18 solarimeter. The sensing element consists of two blackened junctions. The cold junction is in thermal contact with the brass case. The thermopile is covered with two concentric glass hemispherical domes. The response of this instrument is also limited to 0.3 to 3.5 microns. (Platt and Griffiths, 1964).

Net radiation was recorded with a Fritschen minature net radiometer.

The radiometer output is a temperature compensated thermal transducer. The transducer is built with a 22 junction thermopile and a compensating thermistor embedded in epoxy resin. The thermopile is painted with Parsons Black. This unit measures radiation within the wavelength of 0.3 to 50 microns. The wavelength range is limited by its 2 mil polyethylene windows (Fritschen, 1965). The radiometer is shown in Figure 3.6.

Calibration of radiation equipment was done by assuming the calibration of a recently factory calibrated Eppley pyrheliometer to be correct.

Temperature

Temperature profiles were determined with 24 gauge copper-constantan thermocouples constructed with welded junctions. Aspiration was provided to insure representative sampling. Air temperature profiles were obtained within both irrigated sorghum and non-irrigated sorghum canopies. The thermocouples were mounted in an insulated air tower as shown in Figure 3.7 with sampling ports at 20, 40, 80, 160, 240 and 320 cm from the soil surface. Soil temperature profiles in irrigated and non-irrigated regions were taken by placing thermocouples at 2, 4 and 8 cm depths.

Leaf temperatures were determined with thermocouples constructed with 30 gauge wire. Six measurements were made, three of irrigated leaves and three of non-irrigated leaves. The thermocouples were taped to the leaves at the tip, the middle, and close to the stem of the sorghum plant.

Figure 3.6. Fritchen net radiometer in field.

Figure 3.7. Temperature air tower in nonirrigated sorghum.

The thermocouples were referenced with a Joseph Kaye Model 2700 consisting of 24 points whose reference temperature was 65.6°C. This system operates within an ambient temperature range of from -30° to 55°C. It has an ambient temperature sensitivity of less than ± 1°C. over this temperature range. Calibration was accomplished with the use of boiling water and an ice bath. Any thermocouples not in agreement with standard published output were thrown out.

Data Logging

All data except Barnes radiometer and wind data were recorded on a Howell H2812 data logging system as shown in Figure 3.8. The data logging system consists of a digital voltmeter, a scanner, a punch converter, and a paper-tape punch. The system was operated most of the time with a 10-minute interval between scans. The data logger presently has 50 channels with a maximum scan rate of about 3 seconds per channel. The system is capable of accepting sensor outputs in the range from -10 to + 30 millivolts.

The Barnes radiometer data was recorded with a Sargent Model MR recorder as shown in Figure 3.1. The Sargent recorder is a multivoltage recorder with variable chart speed.

Wind System

Wind profile data were obtained with a 6-unit Thornthwaite Model 106 wind profile system. This system has a starting speed of 8.94 cm/sec and a maximum speed of 1450 cm/sec. The system consists of a mast with anemometers located at heights of 20, 40, 80, 160, 240 and 320 cm from the soil surface. The anemometer cups are seven gram conical

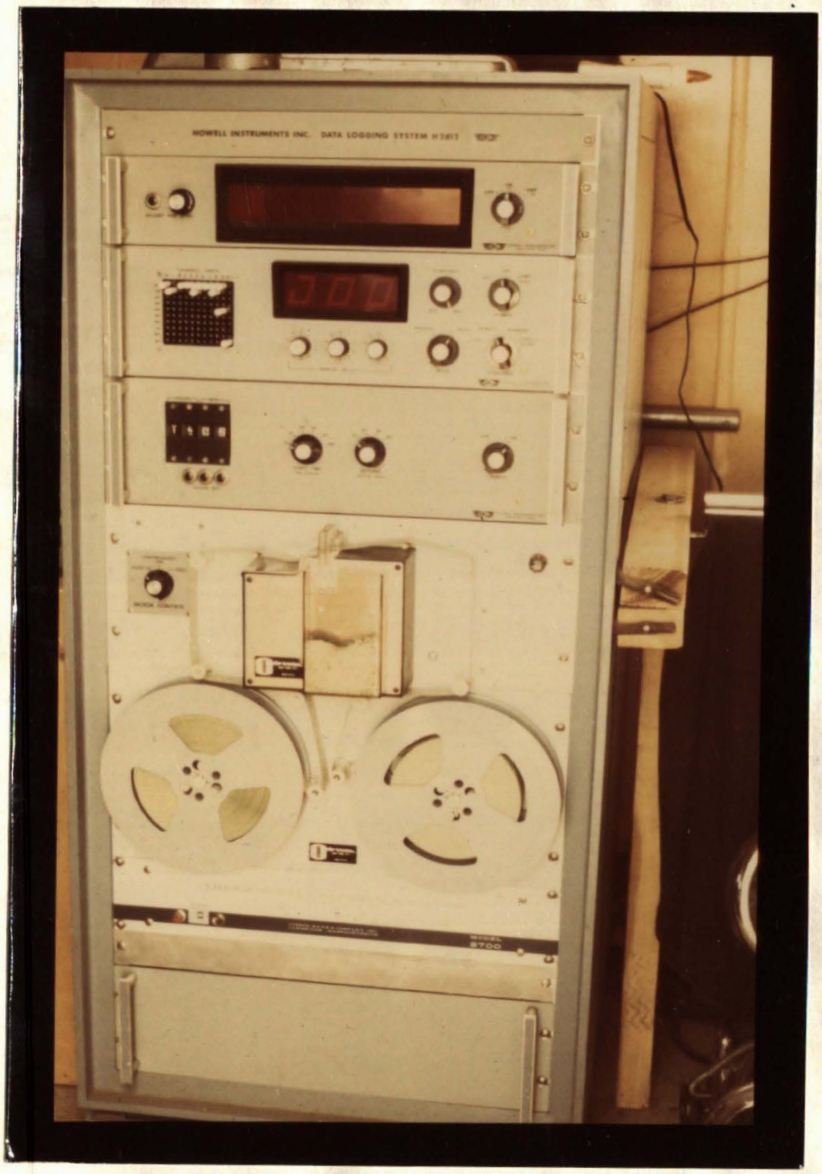


Figure 3.8. Howell data logging system model H2812.

plastic, 5 cm diameter cups with aluminum rings for support.

The output from the anemometers is obtained using a light beam focused on a photo cell. The beam is broken with each revolution of the anemometer. This generates a signal that is recorded on a digital counter. The counter is manually read every half hour.

Soil Heat Flux

The soil heat flux plates used consisted of a glass plate with constantan windings around it. Half of the windings were copper plated. This creates a thermopile which measures the temperature difference normal to the plate. Calibration was obtained with the use of a constant temperature box whose thermal properties were known.

Data Collection Sites and Periods

In an attempt to determine canopy temperature and other microclimate parameters necessary for the calculation of evapotranspiration under actual field conditions data were taken at the James Valley Research and Extension Center.

To do this data were taken on June 23, July 13, 14, 15, 16, 20, 21, 28, 29, August 5, 6, 7, and 16.

The South Dakota State University James Valley Research and Extension Center is located five miles east of Redfield, South Dakota, and one mile north of Highway 212. Irrigation water for the farm is obtained from the James River which is located one-half mile north of the Research Center. Irrigation is accomplished with the use of furrow irrigation. Irrigation and rainfall data for the duration of the study can be found in Figure 3.9.

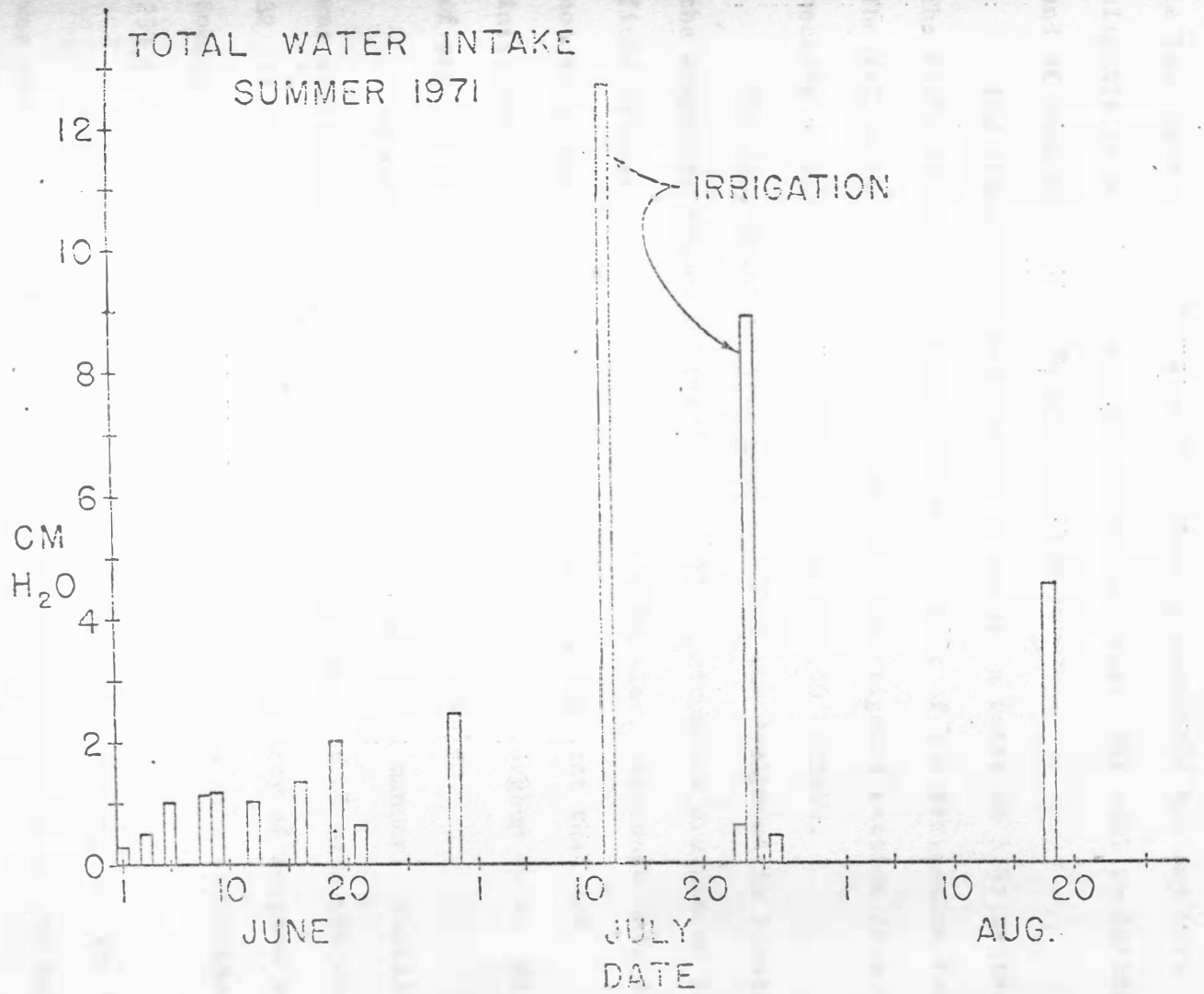


Figure 3.9. Rainfall and irrigation for the summer months.

The soil at the site of the study was Great Bend Silt Loam. The Great Bend Silt Loam is a well-drained friable silty soil that occurs extensively over the Glacial Lake Dakota Plain. The parent material is lake laid silts. This soil is usually permeable and may have slightly to moderately saline parent material. The soil is fertile and of good tilth (Westin et. al., 1954).

The plots shown in Figure 3.10 occupy a total of 3.67 hectares. The field is located in the northeast corner of the irrigation farm. The fallow is a 0.35 hectare plot, the nonirrigated section is a 0.92 hectare plot and the irrigated section is 2.40 hectare.

The instrument trailer used to house the equipment is located in the southwest corner of the fallow. The instruments are placed in the field between 30 and 50 meters from the trailer. Although this does not meet instrument placement requirements, the fact that the instrument site is enclosed on three sides with sorghum in the direction of prevailing winds helps to alleviate this problem.

The seed bed was prepared in a conventional manner. Fertilizer was applied at a rate of 182 Kilograms per hectare of nitrogen and 32 Kilograms per hectare of phosphorus. The variety of sorghum was Sokota 503. The sorghum was planted in 54 cm rows at a population of 250,000 plants per hectare.

Data were taken mostly over the irrigated sorghum, but the scanner was set up in a manner such that it scanned both irrigated and non-irrigated crop.

Placement of instruments can be seen in Figure 3.11.

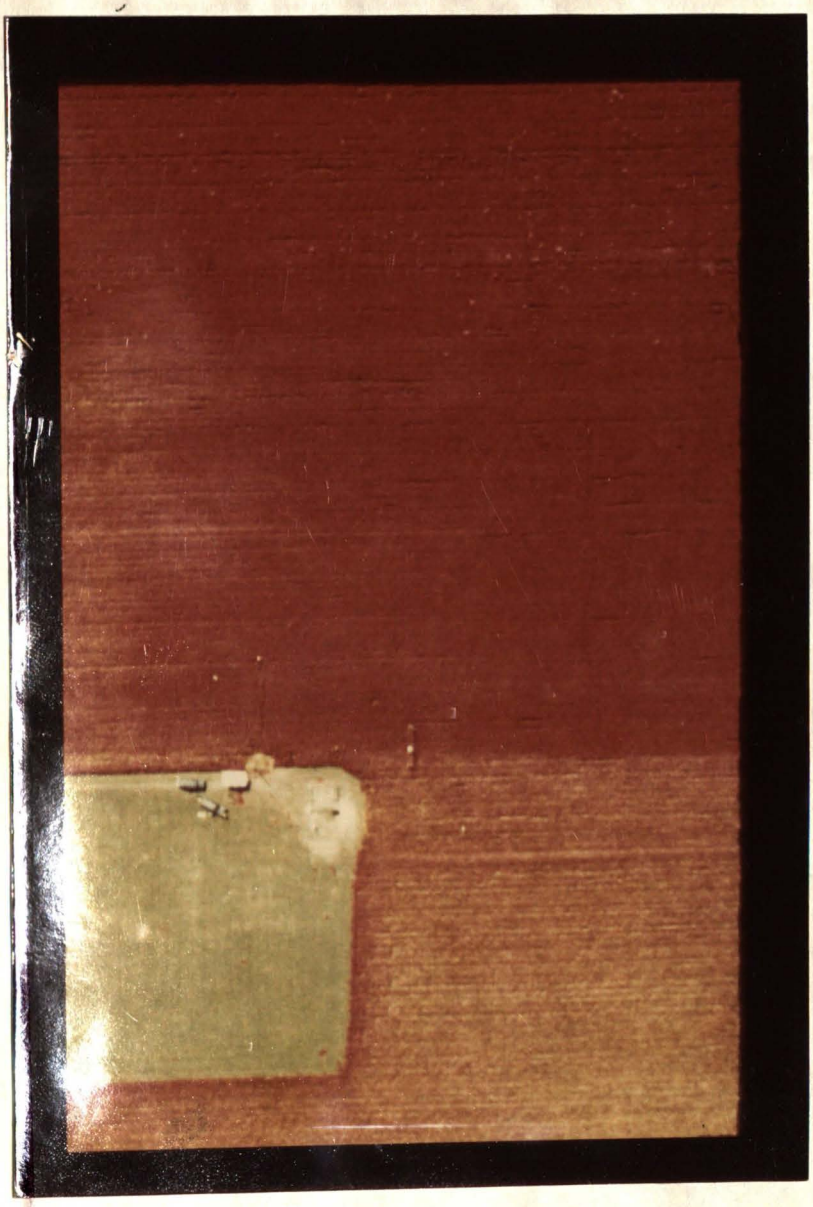

Figure 3.10. Experimental plots, picture taken at 2000 feet on August 16, 1971, with color infrared film. The irrigated shows up darkest red, the non-irrigated is yellow, and the fallow is green.

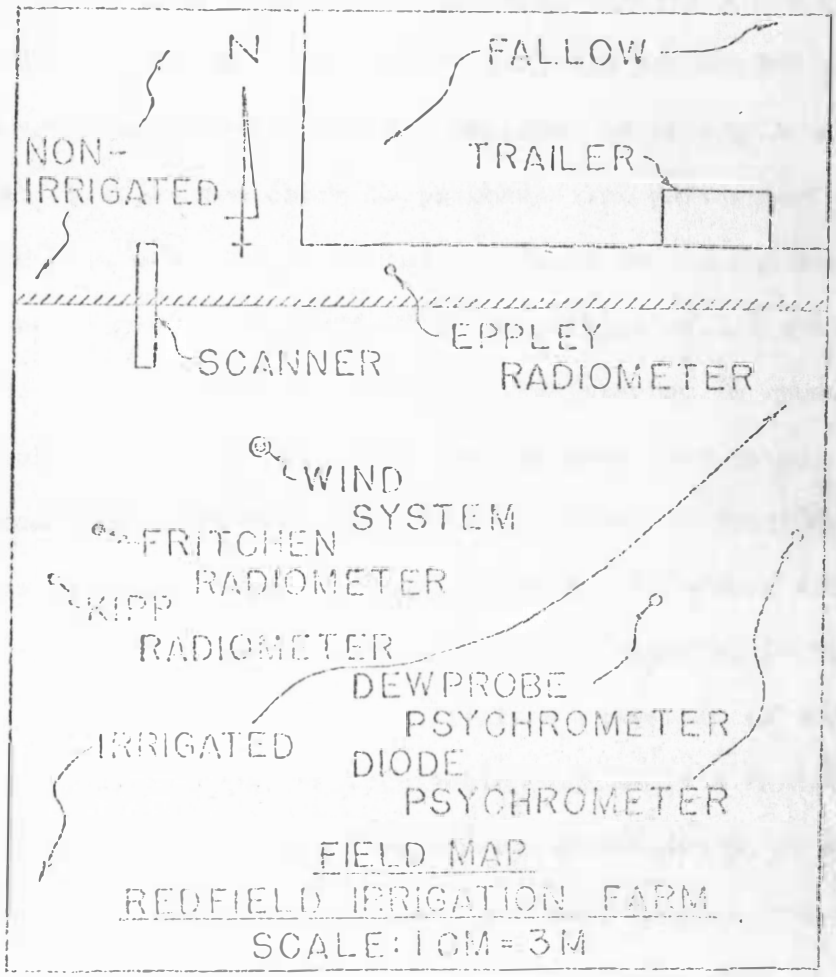


Figure 3.11. Field map showing placement of instruments in sorghum field.

Data Collection and Processing

Data were collected with the Howell data logging system mentioned earlier, which records on paper tape. The paper tape is converted automatically to computer cards at the South Dakota State University Computer Center. The Computer Center utilizes an IBM 360 computer. The cards are then separated by the computer according to channel and another set of separated cards is punched. The particular channels desired are then manually separated according to the desired parameters needed. The program in Appendix I is an example of the several programs written and utilized for this project. The program in Appendix I is a very complete program. It takes the raw data from purely a millivolt output through the different equations necessary to determine evapotranspiration by four different methods. It prints the output of all major parameters and has a plot printout comparing on the same graph the four different evapotranspiration equations as a function of time. It also plots separately radiation values as a function of time. The plot subroutine program was obtained through Share, an organization which distributes programs. It is an extremely useful research tool, but quite inexpensive to utilize. I would estimate that it adds only 30 seconds of running time to a program similar to the one in Appendix I for several hundred sets of data.

## RESULTS AND DISCUSSION

Eight sets of temperature data, collected during the period July 15 through August 7, were used in the analysis. Many more times were attempted but due to weather conditions or mechanical failure the data were not useful.

Some generalities can be drawn from the experimental data. Looking at the difference between the irrigated and nonirrigated sorghum canopy temperatures, as shown in Figures 4.1, 4.3, 4.5, and 4.7, we can conclude that the irrigated sorghum was significantly cooler than the nonirrigated sorghum. This is true for the actively growing portion of the day, probably from 0800 hours to 2100 hours. The difference is usually between 1°C and 2°C; however, differences up to 5°C were recorded on several occasions. When evening comes, this air temperature minus crop canopy temperature trend is reversed.

Another important generality noticed was that in the growth period before heading the air temperature was usually greater than the crop temperature. Between 1800 hours and 2100 hours on days before heading that had an average amount of incoming radiation, the air temperature was 6°C to 9°C greater than was the crop temperature. Between 0600 hours and 0900 hours in the morning, the air temperature was usually 2°C to 3°C higher than the crop canopy temperature.

The plant should be thought of as a system absorbing radiant energy from the sun and emitting energy itself. In its early stages of growth the rapidly developing plant is transpiring a large amount of water. This rapid transpiration rate results in the consumption of the

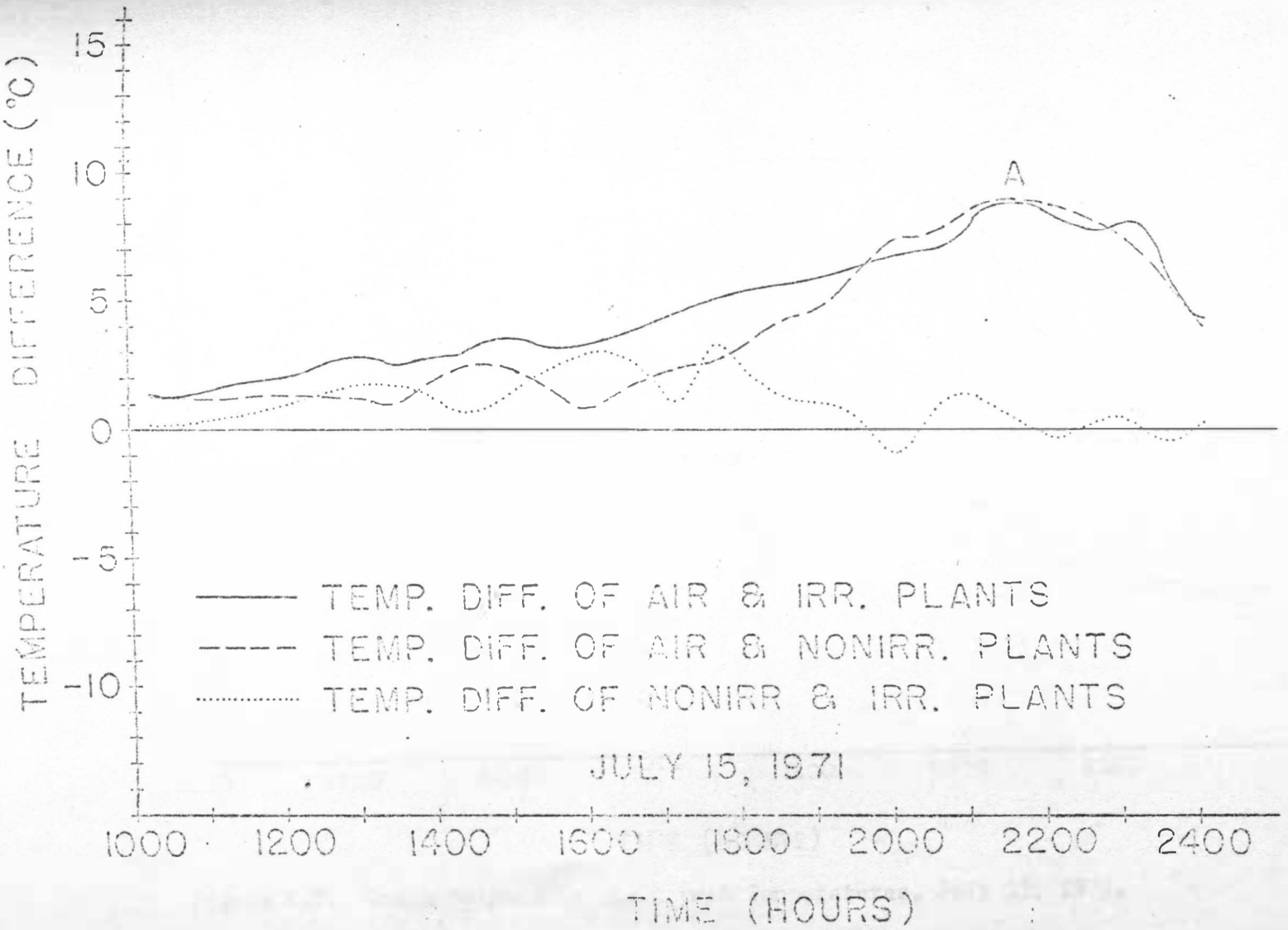


Figure 4.1. Grain Sorghum Canopy Temperature Difference, July 15, 1971.

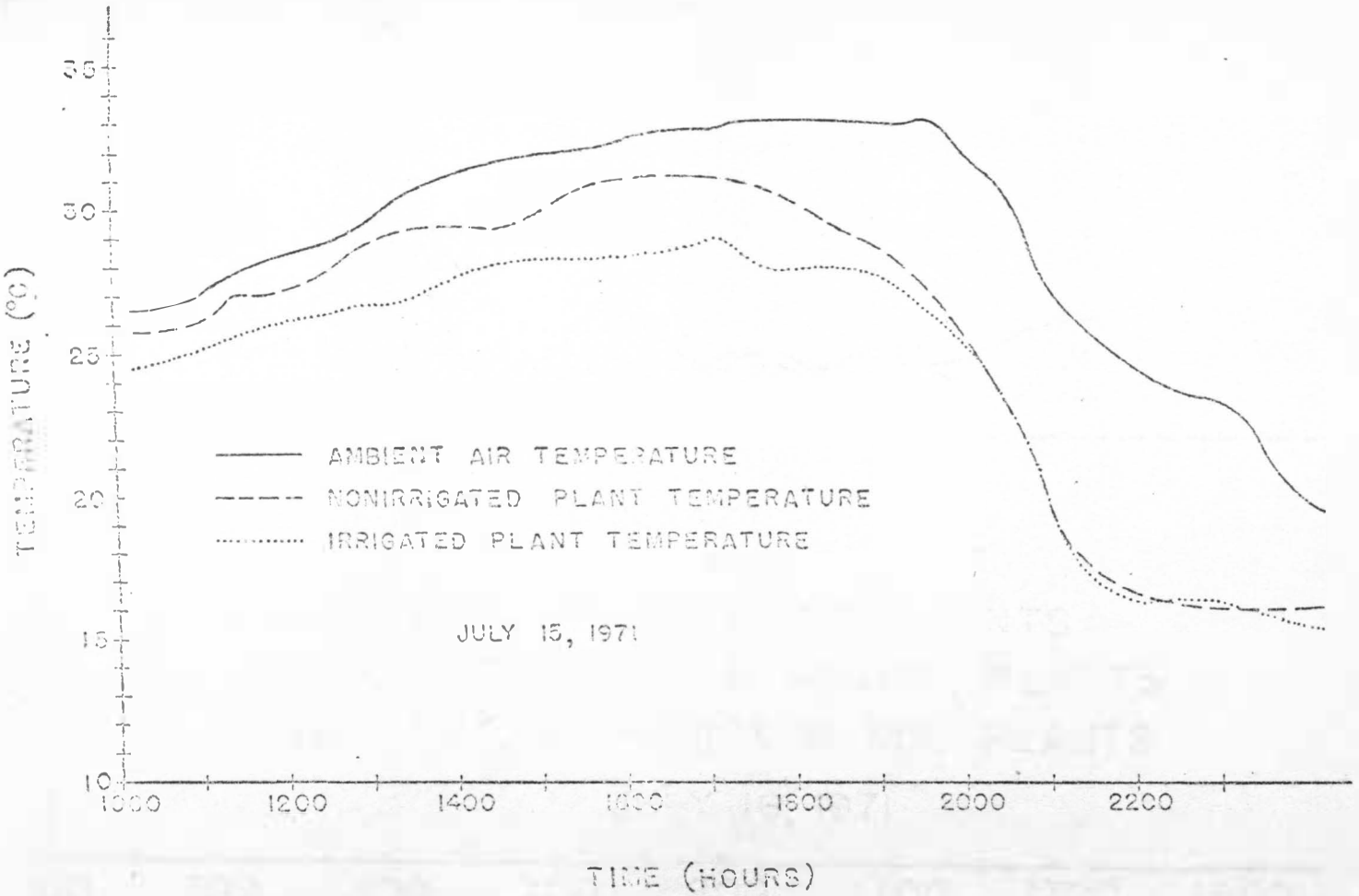


Figure 4.2. Grain Sorghum Canopy Actual Temperatures, July 15, 1971.

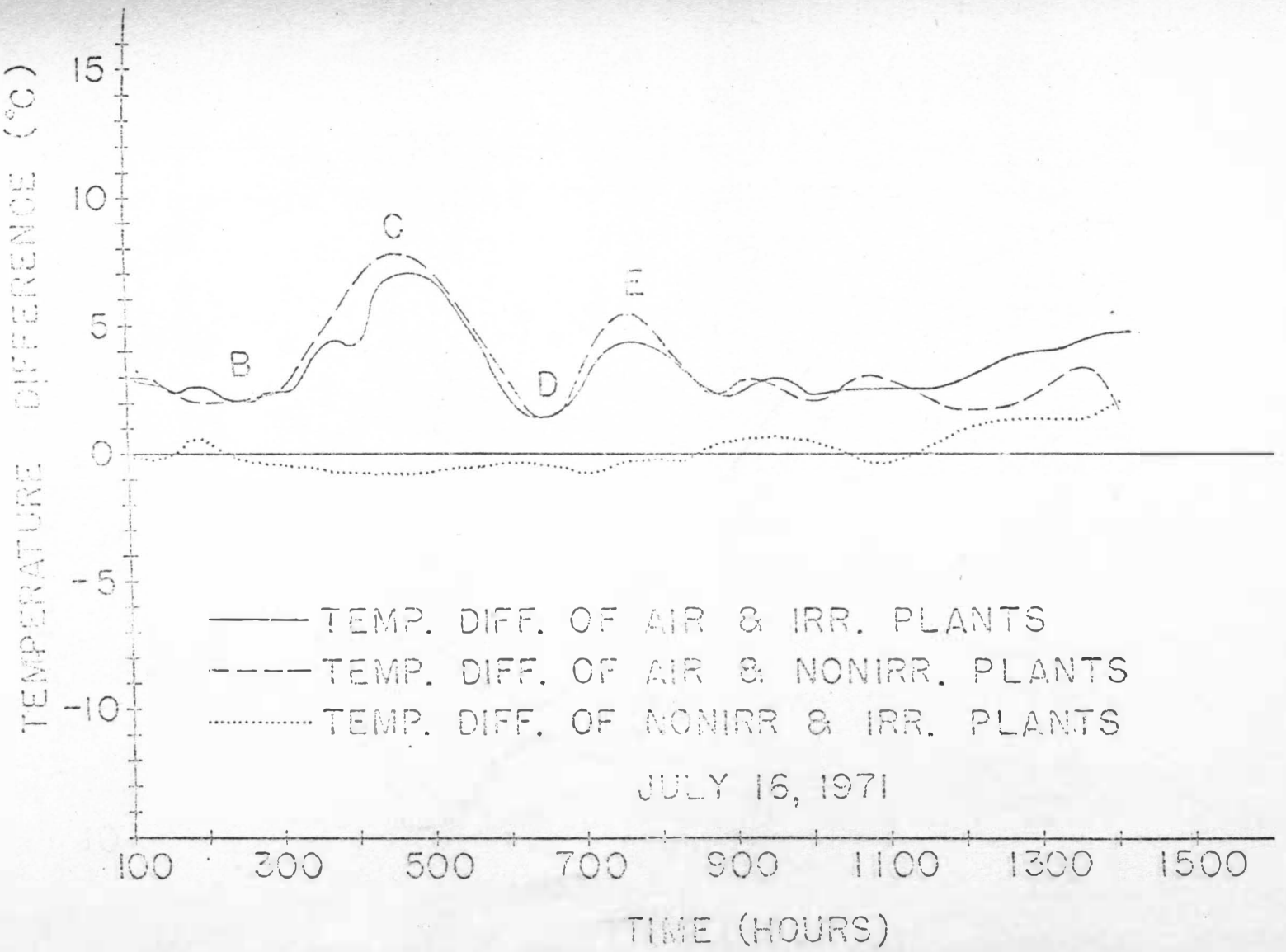


Figure 4.3. Grain Sorghum Canopy Temperature Differences, July 16, 1971.

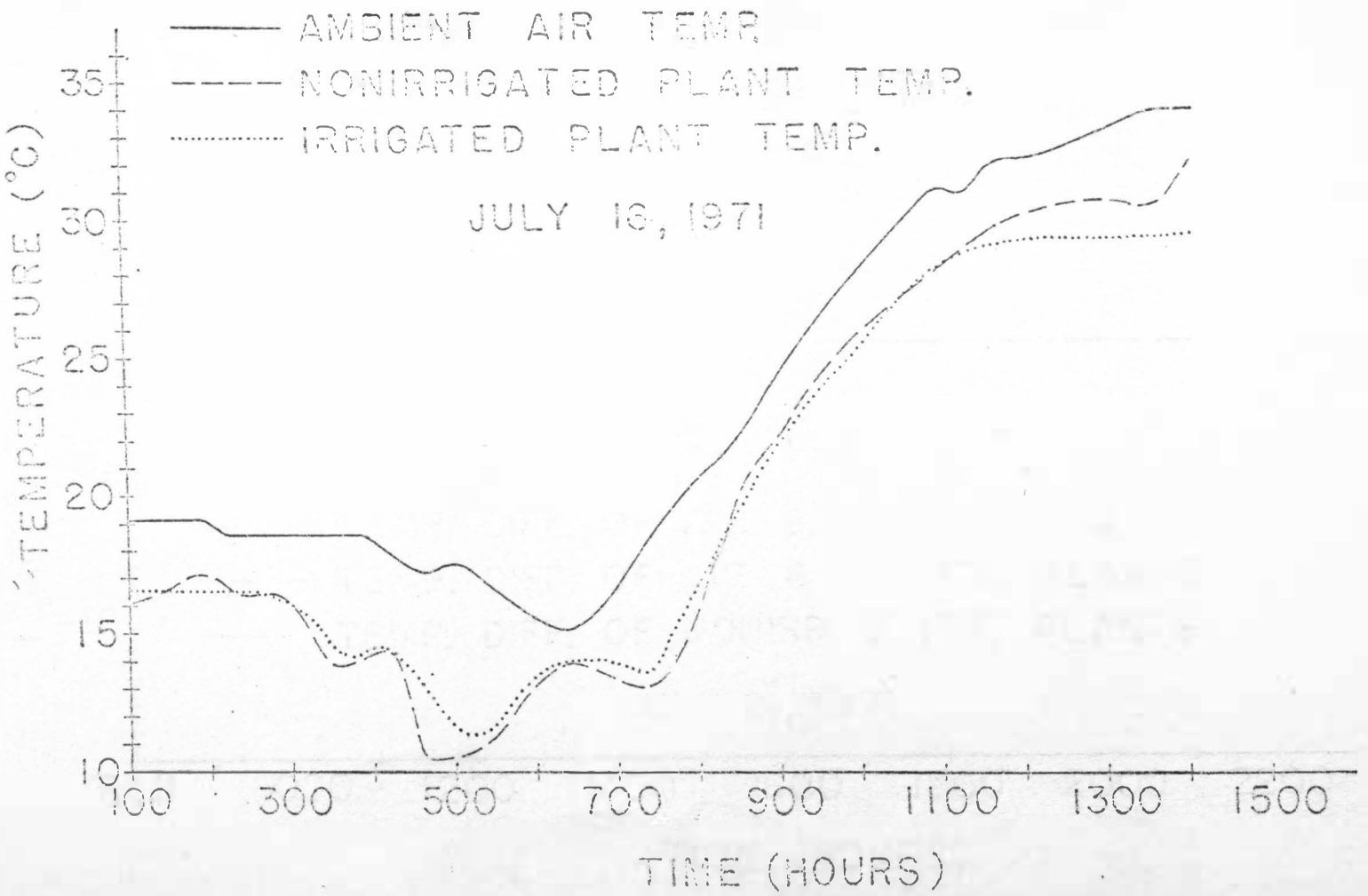


Figure 4.4. Grain Sorghum Canopy Actual Temperatures, July 16, 1971.

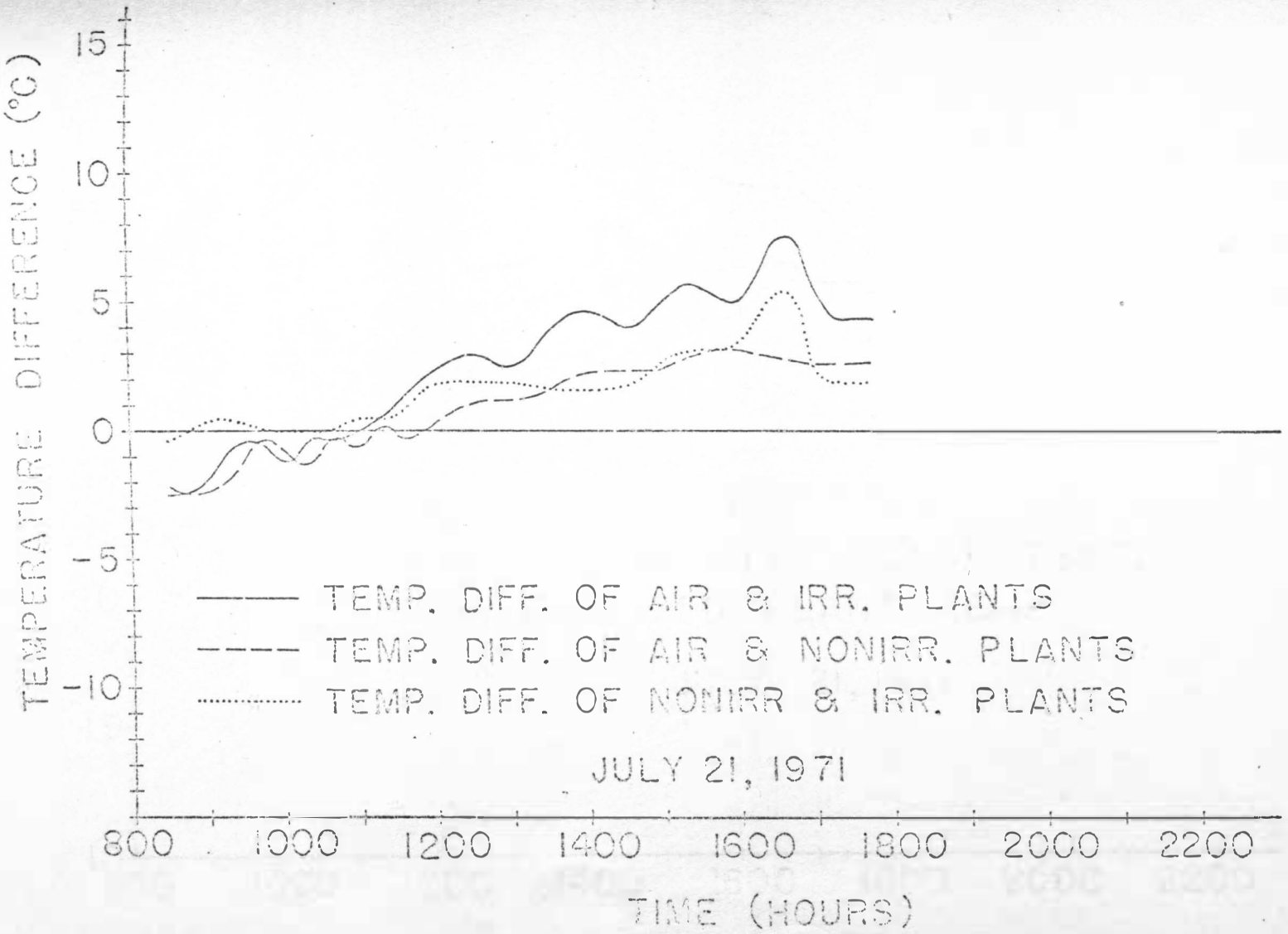


Figure 4.5. Grain Sorghum Canopy Temperature Differences, July 21, 1971.

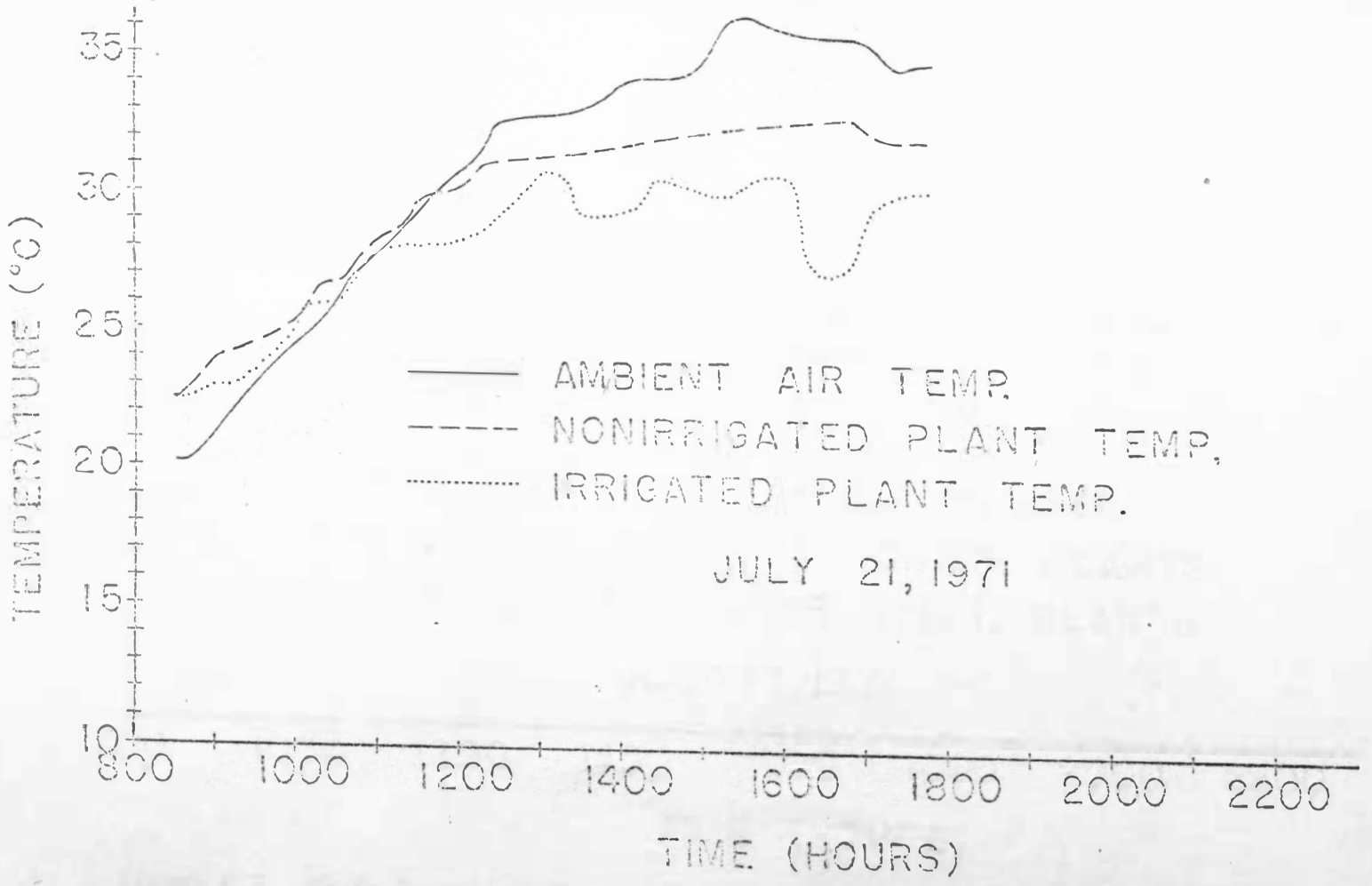


Figure 4.6. Grain Sorghum Canopy Actual Temperature, July 21, 1971.

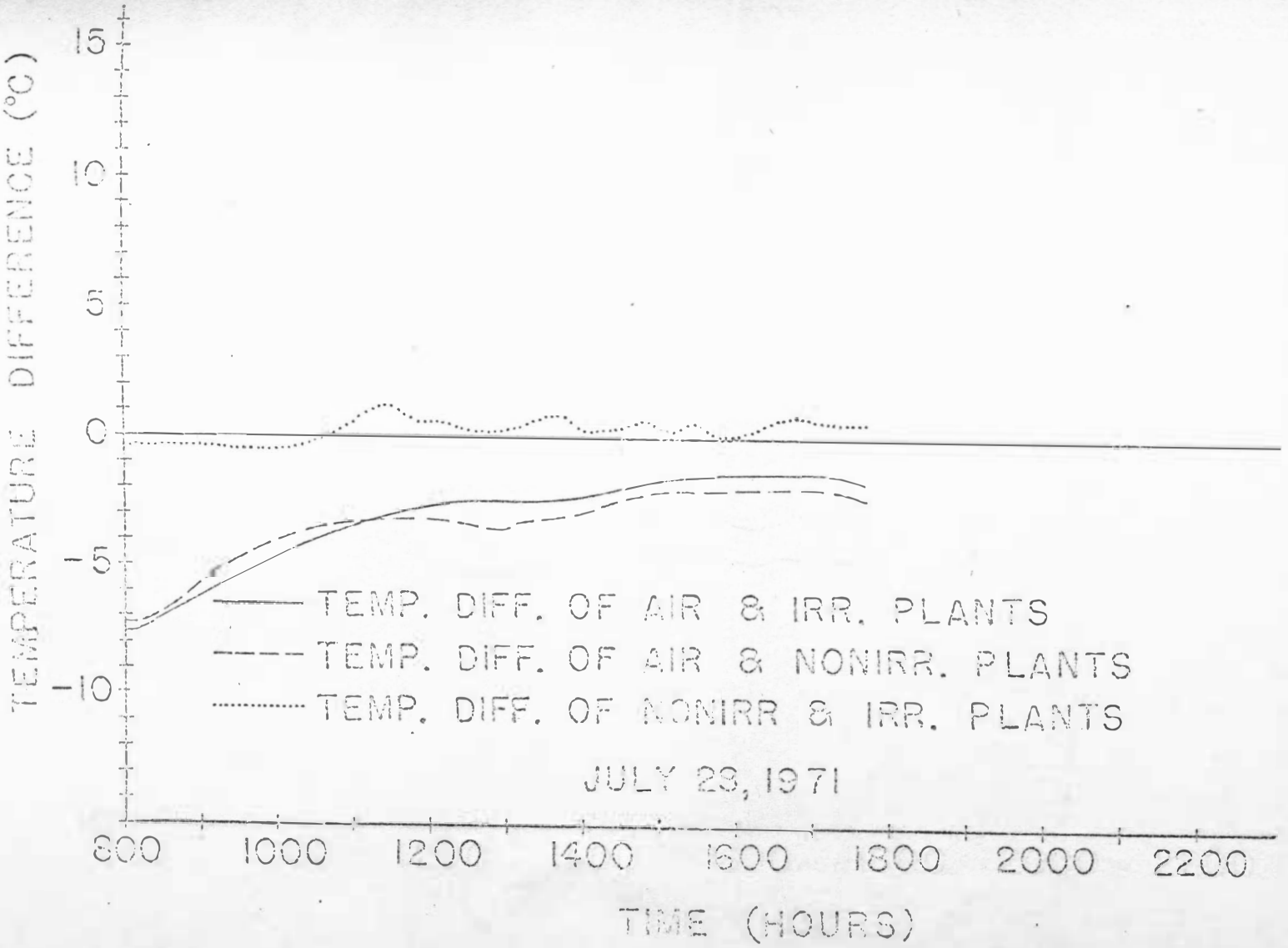


Figure 4.7. Grain Sorghum Canopy Temperature Difference, July 28, 1971.

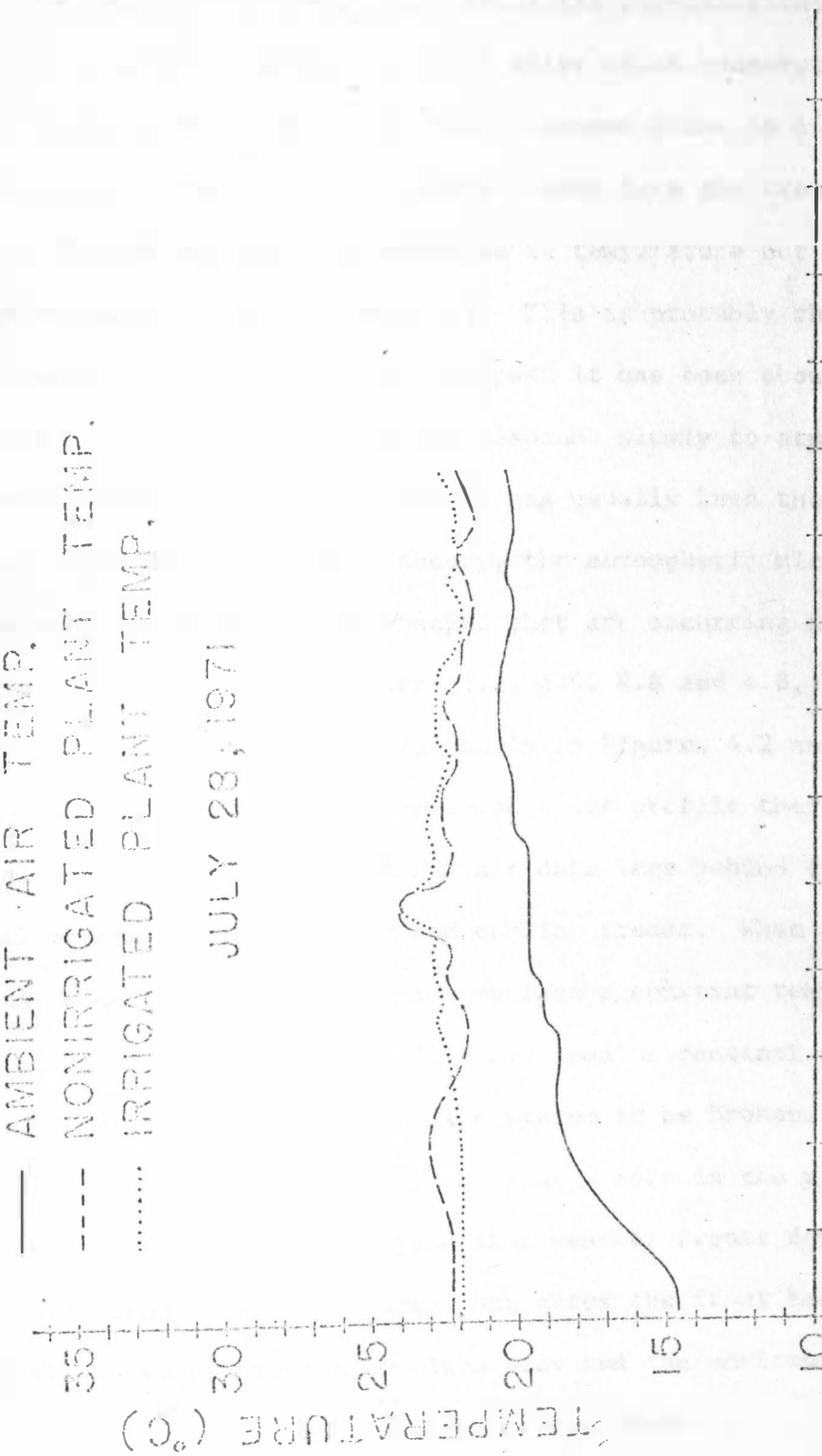


Figure 4.8. Grain Sorghum Canopy Actual Temperatures, July 28, 1971.

plant's thermal energy. The plant temperature is then reduced. The plant, in its continuing attempt to fulfill its physiological needs and maintain a viable temperature, pumps water which evaporates resulting in the plant cooling. As the afternoon draws to a close and evening approaches, the amount of energy coming into the crop system decreases. The air and the crop decrease in temperature but the crop starts its decrease before the air does. This is probably the most important result of this study. In the past it has been thought that the crop behaves much like a heat sink and responds slowly to atmospheric microclimatic changes. Contrary to what has usually been thought and in agreement with Morton's (1969) theory, the atmospheric microclimate around the crop is responding to changes that are occurring in the crop. This is exemplified by Figures 4.2, 4.4, 4.6 and 4.8, but especially the night data of July 15 and 16 in Figures 4.2 and 4.4. For every peak or valley in the crop temperature profile there is a peak or valley in the air data but the air data lags behind the crop data. This occurs in both heating and cooling trends. When an energy equilibrium is established at the crop surface a constant temperature for the air and the crop are created. This remains constant until some force causes the equilibrium of the system to be broken. There are macro-atmospheric conditions that do play a role in the plant-atmosphere system. It can't be argued that weather fronts don't affect the atmospheric conditions of an area, but after the front becomes stationary the above argument comes into play and the environment is affected more by microclimate than by macroclimate.

An interesting and unique set of data was taken on July 15-16. On these two dates, data were recorded continuously from 1000 hours on July 15 to 1400 hours on July 16. Because initial processing gave us the indication that night data showed no significant phenomenon we discontinued on all other runs the taking of data after about 2200 hours in the evening or before 0800 hours in the morning. During the daytime hours of July 15, as shown in Figure 4.2 the mid-afternoon ambient air temperature remained about 33°C. Figure 4.3 shows that the irrigated crop was the usual 1°C cooler than the nonirrigated crop. At about 2230 hours there was a definite reversal of this trend. The nonirrigated sorghum became cooler than the irrigated sorghum. The approximately 1°C cooler nonirrigated temperature remains throughout the night until about 0800 hours of July 16. Figure 4.3 shows that a reversal to the daytime normal trend appears and continues. One possible explanation of these temperature differences lies in the idea that during the daytime the irrigated plant is at a higher water potential. More water requiring less energy is available for the irrigated plant to transpire. It, therefore, remains cooler because the transpiration of greater amounts of water absorbs more energy. As evening approaches the stomata of the plants close, eliminating the transpiration, which was responsible for much of the daytime phenomena. The irrigated crop and soil have a total higher water content which results in the irrigated system having a higher specific heat. It, therefore, cools off slower than the nonirrigated sorghum.

The July 15 and 16 data show interesting deviations of the air temperature from the crop canopy temperature. (When the term, crop

canopy, is used and neither irrigated or nonirrigated is specified, it implies that we are looking at the trend of both surfaces. They follow relatively closely to one another and considering them as a single line when comparing them to air is not inconsistent.) From 1000 hours to 2100 hours, as shown in Figure 4.1, the difference between the ambient air temperature and the canopy temperature rose from 1°C to 9°C. At 2100 hours the curve seems to peak at point A. It then begins a decreasing trend until 2400 hours. In Figure 4.3 of July 16 we see that the curve maintains stability in valley B until about 0300 hours. Here the temperature difference increases until about 0430 hours when it reaches a peak at point C. Proceeding in time we see the difference curves dropping into valley D at about 0630 hours. From there, one more peak, E, is reached before the curve settles down to a rather stable predictable line with about 4°C difference, which was usually the temperature difference between the crop and the air at this time of the day.

Still looking at Figures 4.1 and 4.3, we don't find forthright explanations for all of the peaks and valleys. Peak A is understandable and predictable. It is the culmination of the upward trend of the temperature differences between the air and the plant canopy that is noticeable from the start of the data taking period. Comparing Figures 4.1 and 4.2 it is determinable that peak A, the difference between air temperature and crop canopy temperature,occurs well after the afternoon peaks of the actual crop temperature. Looking at the actual temperature graph, Figure 4.2, we can see that the crop canopy temperature maximum occurred at about 1700 hours. The air temperature

lags behind and doesn't reach a peak until about 2000 hours which again substantiates the theory that the crop reacts to energy imputs, and the atmosphere reacts to the crop. At 1700 hours there was a substantial decrease in incoming radiation. This created a deficit in the canopy sensible heat flux in its equilibrium with latent heat, emitted radiation, reflected radiation, and incoming radiation. This probably resulted from the lack of a sufficient decrease in transpiration; therefore, the latent heat part of the equation assumed a larger percentage of the total. From Figure 4.2 it is reasonable to assume that the reason for the flattening out of the actual crop temperature curve at 2150 hours is because the stomata closed due to insufficient radiation, the temperature gradient became large creating more heat conduction, and the deposition of dew which resulted from the plant remaining at a lower temperature than the air while both the air and the crop concurrently decreased in temperature.

Valley B in Figure 4.3 is a continuation of the bottom of peak A. This level valley is the result of an equilibrium between the plant and its environment. The crop temperature associated with this valley could be at the dew point temperature of the vapor pressure for the air at this point in time. This would be an explanation for the stability of valley B. At 0300 hours on July 16, shown in Figures 4.3 and 4.4, we observed the beginning of a decrease in the crop temperature which is accompanied by peak C, a representation of the air temperature, minus crop temperature, depression, which occurs at 0500 hours. Speculation as to the cause of this decrease in actual temperature, and increase in difference temperature, would be a frontal system moving in bringing

turbulence and air with a lower vapor pressure. This would allow evaporation, causing plant cooling, provide the mechanism for exchange, turbulence, and allow for a lower dew point temperature.

Valley D occurs very close to sunrise. At this time of day there is seldom much turbulence. An increase in incoming energy is also likely. This would cause the increase in canopy temperature between 0500 hours and 0630 hours as seen in Figure 4.4. Peak E probably is the result of turbulence and incoming radiation, evaporating the dew that was known to be present on this particular morning.

Throughout the growing season the air temperature minus a plant temperature function tended to show downward to the right movement, and a decrease in slope. This indicates that as the plant becomes older it tends to more closely reach an equilibrium with the environment around it. In the later stages of the plant's physiological growth, (heading was observed on July 28) the plant temperature was frequently warmer than the ambient air temperature. This is noticeable on the very cold morning of July 28, as shown in Figure 4.8. At 0800 hours on July 28 the ambient air temperature between 14$^{o}$C and 15$^{o}$C. The plants maintained a temperature of about 22$^{o}$C thus showing a large difference between ambient air and plant temperature. Throughout the day of July 28 the maximum ambient air temperature was about 20$^{o}$C. The air temperature was always below the canopy temperature by a difference of at least 2 $^{o}$C. On this particular day the energy imput into the canopy was very low. There are several points in the explanation as to why these results were obtained. First, with such an unusually low temperature the plants' resistance to water flow was probably very high. The high resistance

would cause reduced transpiration and a larger portion of the total incoming radiation would go to the sensible heat flux of the canopy. Secondly, with the air at such a low temperature, a large temperature gradient would exist with the soil acting as a heat source.

The last aspect of canopy temperature which I wish to discuss is illustrated in Figure 4.9. This graph shows fluctuation that can and does occur in the canopy temperature with no significant change in ambient air temperature, if radiation conditions are changed appreciably. This experiment was run on a relatively clear day with one small, but heavy cloud in the sky. The Barnes radiometer was kept stationary and in a position above an irrigated sorghum row. Incoming radiation, air temperature, and crop canopy temperature data were continuously recorded. The results of this experiment indicate a very definite response of the canopy to changes in incoming radiation. They indicate that the plant is very responsive to its environment and responds much more rapidly than the air does to changes in radiation.

In the discussion of evapotranspiration and its determination using meterological parameters, it is first necessary to discuss some of the problems encountered in measurement of parameters.

The accurate measurement of humidity has been a problem to the research worker in the area of climatology for a long period of time. The reason is that a very small change in the actual water content of the air is responsible for a rather large change in relative humidity.

In an attempt to determine the vapor pressure depression between the air layer above the crop and the layer at the crop canopy we utilized two systems. A set of diode psychrometers and a set of dewprobe

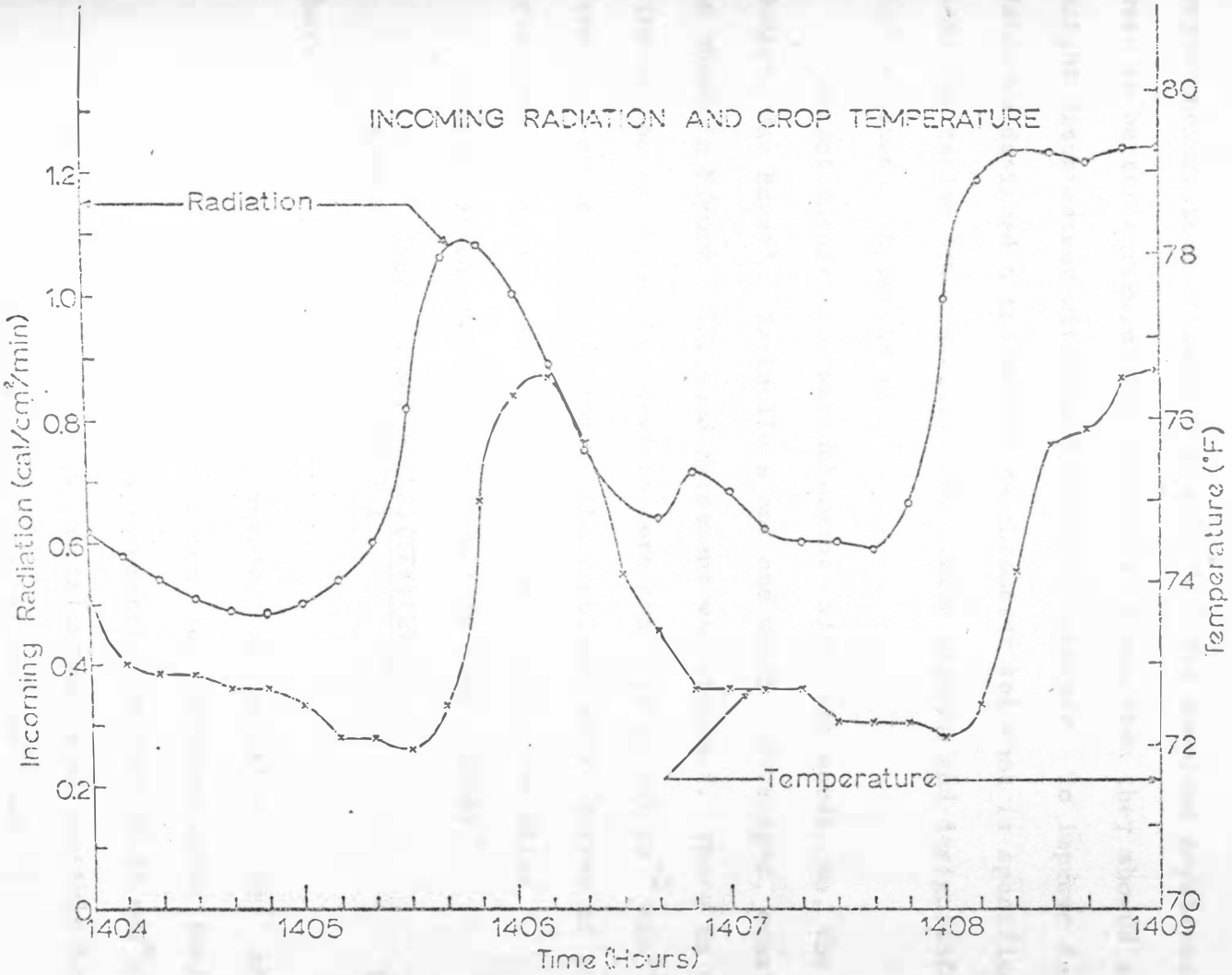


Figure 4.9. Variation in Canopy Temperature with Radiation Changes.

psychrometers. After several sets of data were collected we realized that the diode psychrometers were in very poor agreement with the two Bendix manually operated, wet and dry bulb mercury thermometer psychrometers that we used as standards. The dewprobe psychrometers were in better agreement but there were times when they showed a slight disagreement with the Bendix psychrometer. To improve future data, we designed a thermopile psychrometer set that is specifically made for taking Bowen Ratios. The wiring diagram and design information can be found in Appendix II.

Evapotranspiration was determined with four equations, the Energy Budget, Van Bavel's, Bartholic's and one which I developed, equation 30. As shown in Figure 4.10, good agreement was obtained. There is seldom a time period in which they deviate more than 0.2 gm cal $cm^{-2}$ $min^{-1}$ $gm^{-1}$ from each other. Integration of the resultant daily curves of the four equations would give values that are not greatly dissimilar.

Looking at Van Bavel's equation (Van Bavel, 1966)

$$ETVB = \frac{(SEVT)(HENG) + (LA)(TFC)(EVAD)}{SEVT + 1} \qquad (19)$$

where

ETVB = potential evapotranspiration (gm cal $cm^{-2}$ $gm^{-1}$ $min^{-1}$)

SEVT = slope of the saturation vapor pressure curve (mb/$^{o}$C) divided by the psychrometric constant (0.65 mb/$^{o}$C)

HENG = the sum of energy imputs exclusive of sensible heat and evapotranspiration (gm cal $cm^{-2}$ $gm^{-1}$ $min^{-1}$)

LA = latent heat of vaporization constant (586 cal/cm)

TFC = turbulent transfer coefficient that takes wind into

account for the equation (gm $cm^{-2}$ $min^{-1}$ $mb^{-1}$)

EVAD = saturation vapor pressure deficit of the air above the crop (mb)

We see that Van Bavel uses all of the predominant microclimatic parameters --- radiation, humidity, temperature and turbulence. However, the humidity data that has been used is a vapor pressure deficit at height B above the surface. If there is an error in humidity measurement, it is probably not of a very large relative magnitude because the vapor pressure deficit between saturated vapor pressure and actual vapor pressure is a large difference. In his equation Van Bavel takes into consideration absolute temperature as related to the air's ability to hold moisture by using the slope of the saturation vapor pressure term.

When looking at the data as shown in Figure 4.10, we find that Van Bavel usually has a higher estimation of evapotranspiration than does Bartholic. This is especially true in the early morning period and late evening.

The next equation that I wish to discuss is Bartholic's (1970) equation

$$ETBA = \frac{RFRI + SFLX}{(TDBB - TSF) / (ESB - ESC)} \qquad (20)$$

where

ETBA = potential evapotranspiration by Bartholic (gm cal $cm^{-2}$ $min^{-1}$ $gm^{-1}$)

RFRI = net radiation from Fritschen net radiometer (gm cal $cm^{-2}$ $min^{-1}$ $gm^{-1}$)

SFLX = soil heat flux (gm cal $cm^{-2}$ $min^{-1}$ $gm^{-1}$)

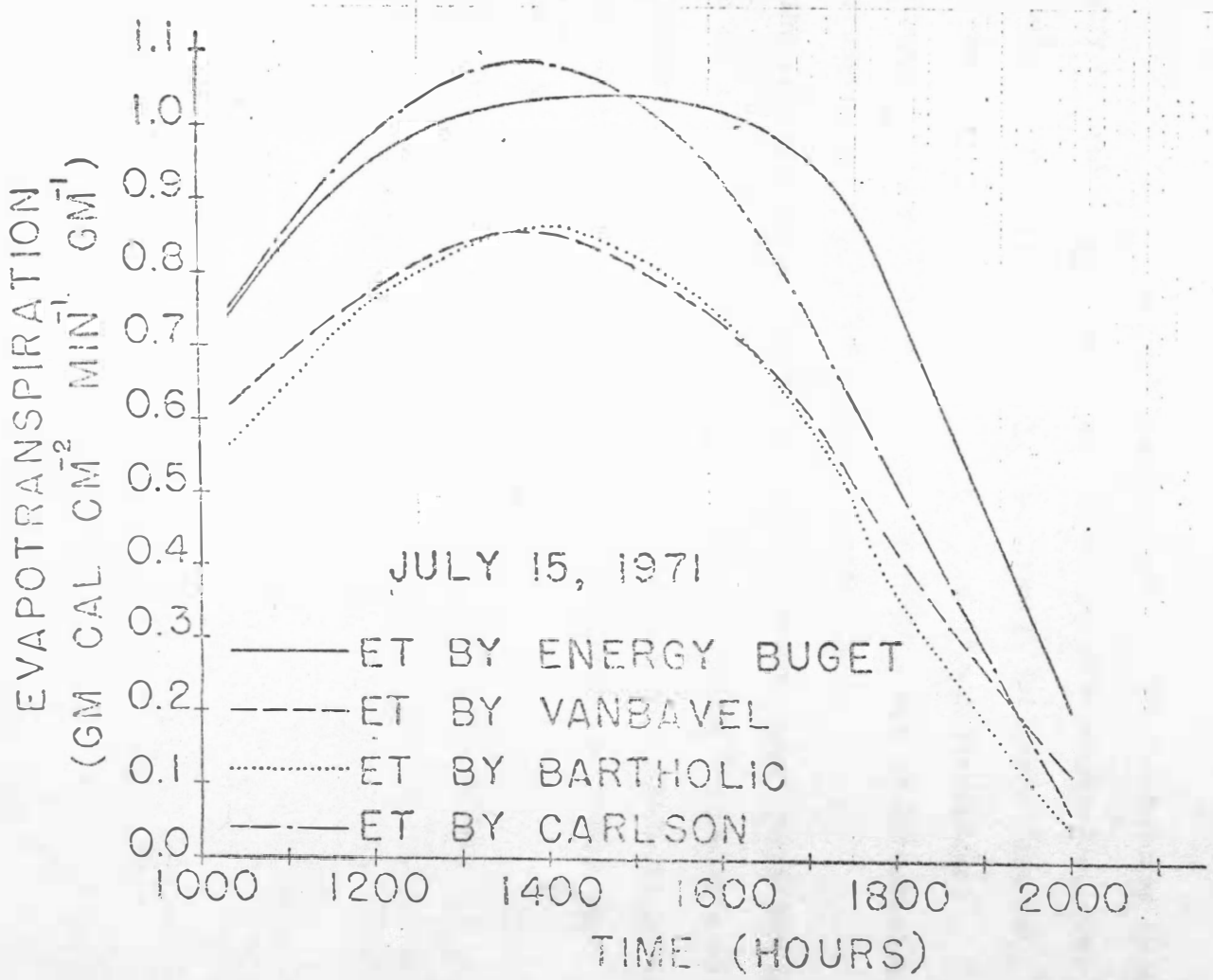


Figure 4.10. ET by Different Equations for July 18, 1971.

TDBB = temperature dry bulb above the surface ($^{o}C$)

TSF = surface temperature as taken with Barnes radiometer ($^{o}C$)

ESB = saturation vapor pressure at temperature TDBB (mb)

ESC = saturation vapor pressure at temperature TSF (mb).

Bartholic's potential evaporation equation is interesting in that basically he uses ambient air temperature, surface temperature, net radiation, and soil heat flux. Below a canopy, soil heat flux is essentially zero and could be neglected. With this assumption, Bartholic has developed an apparently accurate method of determining evapotranspiration with remote sensing parameters.

The data that I have seems to indicate a very good relationship between Bartholic's equation and Van Bavel's although Bartholic's is seldom a higher value than Van Bavel's. Even during periods of little stability Bartholic's equation and Van Bavel's equation follow each other quite closely.

The third equation used was the Energy Balance Equation:

$$ETRN = \frac{RFRI - SFLX}{1 + B} \qquad (21)$$

$$B = .46 \frac{TDBA - TDBB}{EA - EB} \frac{P}{760} \qquad (22)$$

where

ETRN = evapotranspiration by energy balance approach

( gm cal $cm^{-2}$ $min^{-1}$ $gm^{-1}$)

RFRI = net radiation from Fritschen net radiometer

( gm cal $cm^{-2}$ $min^{-1}$ $gm^{-1}$)

SFLX = soil heat flux (gm cal $cm^{-2}$ $min^{-1}$ $gm^{-1}$)

B = Bowen ratio (no units)

TDBA = temperature dry bulb at crop surface height A ($^{o}C$)

TDBB = temperature dry bulb above crop surface height B ($^{o}C$)

EA = vapor pressure at height B (mb)

EB = vapor pressure at height B (mb)

P = atmospheric pressure (mb).

The Energy Balance Equation was the least predictable and least stable of the equations used during the period of comparison. Other scientists have observed similar behavior of the Energy Balance Equation. The results may relate to several reasons. First of all, the measurement of vapor pressure difference between two heights is difficult. A slight error in the measurement of absolute humidity could result in a large error in difference. This is why in our psychrometer design, Appendix II, we utilize the measurements of differences rather than calculating absolute values and then determining differences. Secondly, even if the determination of vapor pressure is correct, it is questionable whether or not this is the value that should be utilized for Bowen's ratio. Bowen (1926) doesn't define his boundaries, but the most accuracy can probably be obtained by utilizing the surface of the crop and a height high enough above the crop canopy so that little change occurs with an increase in height. The upper boundary isn't difficult to define or measure but it is just about impossible to determine vapor pressure right at the crop surface.

In our analysis of the physics of evaporation there are several factors that we realize to be important. In order for water to change

states, from a liquid to a vapor, three physical conditions must be met. There must be sufficient energy available, a negative vapor pressure gradient must exist, and water must be available to be evaporated. In an attempt to derive a workable evapotranspiration equation, these factors must provide the theoretical basis.

Under irrigated field conditions water is seldom a limiting factor. This leaves two conditions to be satisfied. They can be expressed in the following equation:

$$ET = f(RNET, ES) \tag{23}$$

where

ET = evapotranspiration (gm cal $cm^{-2}$ $min^{-1}$ $gm^{-1}$)

RNET = net radiation ( gm cal $cm^{-2}$ $min^{-1}$ $gm^{-1}$)

ES = vapor pressure gradient (mb).

Another assumption that I have made is that when a crop has no water deficit and is rapidly transpiring, the air in contact with the crop canopy is at its saturation vapor pressure. The air in the vicinity of the crop is also close to being saturated; therefore, both the vapor pressure of the crop and the vapor pressure of the air can be determined by their respective temperatures. The vapor pressure gradient then becomes a function of the temperature differences of the air and the crop. This would make the determination of evapotranspiration by parameters of remote sensing possible.

In an attempt to determine a realistic approximation of evapotranspiration using remote sensing parameters, I tried many methods of analysis and derivation. The equation which I finally considered to be the most physically sound resulted from the combination of two existing rather

sound equations. The first is Sheppard's (1958) Equation.

$$ET = \frac{(WMOL)(DENA)(CVK)(HTCON)(EB - EA)(586)}{(P)\quad (Ln((CVK)\ (HTCON)\ (ZB)/(D)))} \tag{24}$$

where

ET = evapotranspiration by Sheppard (gm cal $cm^{-2}$ $min^{-1}$ $gm^{-1}$)

WMOL = ratio of molecular weight of water to molecular weight of air (0.622)

DENA = density of air ($1.168 \times 10^{-3}$ $gm/cm^3$)

CVK = Van Karman's constant (41)

HTCON = friction velocity constant

EB = vapor pressure above the surface (mb)

EA = vapor pressure at the surface of the crop (mb)

P = air pressure (mb)

ZB = height above crop surface (cm)

D = diffusivity of water vapor in air (0.25 $cm^2/sec$).

The second equation is the Energy Budget Equation:

$$RNET = SFLX + A + ET + PH + M \tag{25}$$

where

RNET = net radiation (all units in gm cal $cm^{-2}$ $min^{-1}$ $gm^{-1}$)

SFLX = soil heat flux

A = canopy heat flux and air heat flux

ET = evapotranspiration

PH = energy consumed in photosynthesis

M = miscellaneous term.

For a canopy surface it is consistent to assume SFLX, PH, and M to be insignificant. These terms will usually amount to less than the

error found in measuring RNET. We can, therefore, conclude that:

$$RNET = A + ET. \tag{26}$$

Bowen's ratio states:

$$B = \frac{A}{ET} = (6.05)(10^{-4}) \left[\frac{TDBB - TSF}{EA - EB}\right] (P) \tag{27}$$

The Bowen ratio is changed slightly from the way it first appears. The original equation used the term TDBA rather than TSF. TSF is a more realistic and exact estimate of the parameter measured. The reason TSF has not been used in the past is because of the difficulty in trying to measure it. Until thermal radiometers came into use it was practically impossible.

By rearranging terms we get:

$$EA - EB = \frac{6.05 \times 10\ (TDBB - TSF)(P)}{RNET/ET - 1} \tag{28}$$

Substitution of (28) into (24) gives:

$$ET = \frac{(WMOL)(DENA)(CVK)(HTCON)(586)(6.05)(10^{-4})(TDBB - TSF)}{\frac{RNET}{ET} - 1 \qquad \ln \frac{(CVK)(HTCON)(ZB)}{D}} \tag{29}$$

$$ET = \frac{RNET - (WMOL)(DENA)(CVK)(HTCON)(586)(6.05 \times 10^{-4})(TDBB - TSF)}{\ln((CVK)(HTCON)(ZB)/D)}$$

Upon looking at the data, Figure 4.10, we find that this equation gives results that are at times 0.1 to 0.2 gm cal $cm^{-2}$ $min^{-1}$ $gm^{-1}$ higher than Van Bavel's or Bartholic's. The reason for this, I belive, lies in the convection constant, HTCON. An increase in the HTCON constant would decrease ET. The greatest decrease would come on windy days.

Theoretically

$$HTCON = \frac{CVK\ (WSPDB - WSPDA)}{\ln\ (ZB/ZA} \qquad (31)$$

where

WSPDA = wind speed at heights ZA

WSPB = wind speed at height ZB.

Because of the logarithmic nature of wind profiles HTCON will usually remain relatively constant for one particular ground surface. For our work I chose 0.008 which, from the results, seems to be too small. More work is being done to determine what an accurate estimation of this figure would be for different crop surfaces.

# SUMMARY, CONCLUSIONS, AND SUGGESTIONS FOR FUTURE WORK

During the growing season there are definite trends and patterns that are followed by the plant in its reaction to climatological conditions. In our work, air temperature minus sorghum temperature was usually positive during the early part of the growing season. After heading, the sorghum tended to be warmer than the air in the early morning and on cold days. I have speculated that this was either the result of physiological changes in the plant or a greater ambient air temperature fluctuation that occurred as the plants approached maturity. More work is needed to determine the cause of this change in the plant canopy, temperature pattern. The phenomena observed by taking night temperature data were interesting and deserve more study.

Thermal imagery has many possibilities for remote sensing of ground conditions. In order to obtain valid results, climatological parameters that affect the crop must be considered. It is possible that the crop canopy temperature is a function of both soil, and physiological conditions which would include water content, nutrient status, insect infestations, and disease. However, it is also a function of the total daily integrated potential evapotranspiration that has occurred on that particular day up to the time being considered. This hypothesis is substantiated to a limited extent by my thesis work and is further exemplified by the work of Cary and Wright (1971) who have stated that plant water potentials are generally more closely correlated to potential evapotranspiration than to soil water content. The last two statements are not meant to imply that soil water, nutrient status, and physiological conditions of the plant can not be determined with

remote sensing techniques. However, the applications of remote sensing are dependent upon an understanding of the interactions of soil, plant, and meteorological conditions near the earth's surface. If we understand these interactions, we can eliminate the effect of meteorological conditions and obtain useful soil and plant data.

In determination of evapotranspiration under field conditions, more work is needed in evaluation of the accuracy of presently used and accepted equations and in extending their application to a regional basis. I believe that regional evapotranspiration from irrigated crop land can be accurately determined with remote sensing parameters. Because of complications, more information is needed to determine if evapotranspiration from dry land conditions can be determined by remote sensing.

This work, although utilizing ground based remote sensors has its most far reaching applications in aerial remote sensing. We found from observations of the plant, that its emitted thermal spectrum showed changes and variation related to changes in the environment. From these observations, I suggest that the same type of response might occur in other spectral imagery. In the future, it is imperative that the plant be thought of as the dynamic system which it is, reacting rapidly and responsively to its environment.

# LIST OF REFERENCES


1. Bartholic, J. F., L. N. Namken, and C. L. Wiegand. 1970. Combination equations used to calculate evapotranspiration and potential evapotranspiration. Agricultural Research Service. ARS 41-170.

2. Bowen, J. S. 1926. The ratio of heat losses by conduction and by evaporation from any water surface. Physical Review, 27:779-787.

3. Buettner, K.J.K., and C. D. Kern. 1965. The determination of infrared emissivities of terrestrial surfaces. Journal of Geophysical Research, 70:1329-1337.

4. Cary, J. W. and J. L. Wright. 1971. Response of plant water potential to the irrigated environment of southern Idaho. Agronomy Journal, 63:691-695.

5. Conaway, J. and C.H.M. Van Bavel. 1967. Evaporation from a wet soil surface calculated from radiometrically determined surface temperatures. Journal of Applied Meterology, 6:650-655.

6. Coulson, K. L. 1966. Effects of reflection properties of natural surfaces in aerial reconnaissance. Applied Optics, 5:905-917.

7. Denmead, O. T. and R. H. Shaw. 1962. Availability of soil water to plants as affected by soil moisture content and meteorological conditions. Agronomy Journal, 54:385-390.

8. Feagle, R. G. and J. A. Businger. 1963. An Introduction to Atmospheric Physics. Academic Press, New York and London.

9. Fritschen, L. J. 1965. Miniature net radiometer improvements. Journal of Applied Meteorology, 4:528-532.

10. Fuchs, M. and C. B. Tanner. 1966. Infrared thermometry of vegetation. Agronomy Journal, 58:597-601.

11. Gardner, W. R. 1965. Dynamic aspects of soil-water availability to plants. Annual Review of Plant Physiology, 16:323-342.

12. Gates, D. M. 1963. Leaf temperature and energy exchange. Archives of Meteorological Physics, 12:321-336.

13. Gates. D. M. 1964. Leaf temperature and transpiration. Agronomy Journal, 56:273-277.

14. Gavande, S. A. and S. A. Taylor. 1967. Influence of soil water potential and atmospheric evaporative demand on transpiration and the energy status of water in plants. Agronomy Journal. 59:4-7.

15. Horton, M. L., L. M. Namken, and J. T. Ritchie. 1970. Role of plant canopies in evapotranspiration. Evapotranspiration in the Great Plains. Agricultural Experiment Station, Kansas State University, Manhattan, 301-339.

16. Idso, S. B., D. G. Baker, and D. M. Gates. 1966. The energy environment of plants. Advances in Agronomy. 18:171-216.

17. Idso, S. B., and D. G. Baker. 1967. Method of calculating the photosynthetic response of a crop to light intensity and leaf temperatures by an energy flow analysis of the meteorological parameters. Agronomy Journal. 59:13-21.

18. Jackson, R. D., and S. B. Idso. 1969. Ambient temperature effects in infrared thermometry. Agronomy Journal. 61:324-325.

19. LaRue, M. E., D. R. Nielsen, and R. M. Hagan. 1968. Soil water flux below a ryegrass root zone. Agronomy Journal. 60:625-629.

20. Millington, R. J. and D. B. Peters. 1970. Transport in the soil-plant-atmosphere continuum. Scientia. 64:26-51.

21. Monteight, J. L. 1965. Evaporation and environment. 205-234. The State and Movement of Water in Living Organism. Academic Press, New York.

22. Monteith, J. L. and G. Szeicz. 1962. Radiative temperature in the heat balance of natural surfaces. Quarterly Journal of the Royal Meteorological Society. 88:496-507.

23. Morton, F. I. 1969. Potential evaporation as a manifestation of regional evaporation. Water Resources Research. 5:1244-1255.

24. Platt, R. B., and J. F. Griffiths. 1964. Environmental Measurement and Interpretation. Reinhold Publishing Corperation, New York.

25. Rose, C. W. 1969. Agricultural Physics. Pergamon Press, London, New York, Paris.

26. Rosenberg, N. J., E. H. Hoyt, and K. W. Brown. 1968. Evapotranspiration. MP20 University of Nebraska College of Agriculture and Home Economics.

27. Sheppard, P. A. 1958. Transfer across the earth's surface and through the air above. Quarterly Journal of the Royal Meteorological Society. 84:205-224.

28. Shortley, G., and D. W. Williams. 1958. Elements of Physics. Prentice-Hall Incorporated, Englewood Cliffs, New Jersey.

29. Slatyer, R. O., C. E. Hounam, K. C. Leverington, and W. C. Swinbank. 1970. Estimating evapotranspiration. Australian Water Resources Council, Hydrological Series, Number 5. Department of National Development, Canberra, Australia.

30. Sutton, O. G., 1953. Micrometeorology. McGraw-Hill Book Company, New York.

31. Tanner, C. B., and M. Fuchs. 1968. Evaporation from unsaturated surfaces: A generalized combination method. Journal of Geophysical Research. 73:1299-1304.

32. Tanner, C. B., and W. L. Pelton. 1960. Potential evapotranspiration estimates by the Approximate Energy Balance method of Penman. Journal of Geophysical Research. 65:3391-3413.

33. Van Bavel, C. H. M. 1966. Potential evaporation: The combination concept and its experimental verification. Water Resources Research. 2:455-467.

34. Van Wijk, W. R. 1963. Physics of Plant Environment. North Holland Publishing Company, Amsterdam.

35. Westin, F. C., G. J. Buntley, W. C. Moldenhauer, and F. E. Shubeck. 1954. Soil Survey of Spink County. Bulletin Number 439. Agricultural Experiment Station. South Dakota State University.

36. Wiegand, C. L., and L. N. Namken. 1966. Influences of plant moisture stress, solar radiation, and air temperature on cotton leaf temperature. Agronomy Journal. 58:582-586.

# APPENDIX I

## EVAPOTRANSPIRATION COMPUTER PROGRAM

```
0001            DIMENSION HEAD(200),ORD(200),ABSC(200),HEADA(200),ORDA(200)
0002            DIMENSION TDPAF(200),TDPA(200),TDPBF(200),TDPB(200),EA(200)
0003            DIMENSION EB(200),ESA(200),ESB(200),RERI(200),RERIA(200)
0004            DIMENSION RNET(200),RSOLA(200),RSOL(200),ROUTA(200),B(200)
0005            DIMENSION NTIME(200),TDBAA(200),TDBA(200),TDBBA(200),TDBB(200)
0006            DIMENSION SELXA(200),SELX(200),RHA(200),RHB(200),ALEB(200)
0007            DIMENSION ETRN(200),ROUT(200),TDBAK(200),TDBBK(200),TDPAK(200)
0008            DIMENSION TDPBK(200),EVAP(200),HEAG(200),TSF(200),TSFA(200)
0009            DIMENSION TEVT(200),SEVT(200),TFC(200),WSPDB(200),ZC(200)
0010            DIMENSION XTIME(200),XHOUR(200),XMINT(200),EE(200),ETBA(200)
0011            DIMENSION ETVB(200),SLOPE(200),HTP(200),WSPDA(200),DISP(200)
0012            DIMENSION ESC(200),TSFKK(200)
0013            DATA ORD(1)/'    '/,ORD(2)/'    '/,ORD(3)/'    '/,ORD(4)/'    '/,O
                1RD(5)/'    '/,ORD(6)/'    '/,ORD(7)/'    '/,ORD(8)/'CAL '/,ORD(9)/
                2'CME2'/,ORD(10)/' MIN'/
0014             DATA HEAD(1)/'    '/,HEAD(2)/'    '/,HEAD(3)/'    '/,HEAD(4)/'
                1'/,HEAD(5)/'    '/,HEAD(6)/'    '/,HEAD(7)/'    '/,HEAD(8)/'    '/
                2,HEAD(9)/'    '/,HEAD(10)/'    '/,HEAD(11)/'    '/,HEAD(12)/'   T'
                3/,HEAD(13)/'EMPE'/,HEAD(14)/'RATU'/,HEAD(15)/'RE V'/,HEAD(16)/'S T
                4I'/,HEAD(17)/'ME P'/,HEAD(18)/'LOT '/
0015             DATA ABSC(1)/'    '/,ABSC(2)/'    '/,ABSC(3)/'    '/,ABSC(4)/'
                1'/,ABSC(5)/'    '/,ABSC(6)/'    '/,ABSC(7)/'    '/,ABSC(8)/'    '/
                2,ABSC(9)/'    '/,ABSC(10)/'    '/,ABSC(11)/'    '/,ABSC(12)/'    '
                3/,ABSC(13)/'    '/,ABSC(14)/'    '/,ABSC(15)/'  FI'/,ABSC(16)/'ME
                4 '/
0016             DATA HEADA(1)/'    '/,HEADA(2)/'    '/,HEADA(3)/'    '/,HEADA(4)/'
                2    '/,HEADA(5)/'    '/,HEADA(6)/'    '/,HEADA(7)/'    '/,HEADA(8)
                3/'    '/,HEADA(9)/'    '/,HEADA(10)/'    '/,HEADA(11)/'   R'/,HEAD
                4A(12)/'ADIA'/,HEADA(13)/'TION'/,HEADA(14)/' VS '/,HEADA(15)/'TIME'
                8/
0017             DATA ORDA(1)/'    '/,ORDA(2)/'    '/,ORDA(3)/'    '/,ORDA(4)/'
                5'/,ORDA(5)/'    '/,ORDA(6)/'    '/,ORDA(7)/'    '/,ORDA(8)/'    '/
                6,ORDA(9)/'    '/,ORDA(10)/'   R'/,ORDA(11)/'ADIA'/,ORDA(12)/'TION'
                7/
0018             1 FORMAT(I5,1X,I3,6F4.0)
0019            10 FORMAT(8(1X,F2.0,F2.0,1X,F4.1))
0020            11 FORMAT(8(1X,I4,1X,F4.2))
0021            12 FORMAT(8(1X,I4,1X,F4.1))
0022            13 FORMAT(8(1X,I4,1X,F4.1))
0023            20 FORMAT(8(1X,I4,F5.0))
0024            19 READ(11,1)NDATE,M,XMIN,XMAX,YMIN,YMAX,YMI,YMA
0025               IF(M-200)99,50,50
0026            99 CONTINUE
0027               READ(11,10)(XHOUR(I),XMINT(I),TDPAF(I),I=1,M)
                C     TDPAF = TEMPERATURE DEW POINT DEGREE F AT SURFACE
0028               READ(11,13)(NTIME(I),TDPBF(I),I=1,M)
                C     TDPBF = TEMPERATURE DEW POINT DEGREE F ABOVE SURFACE
0029               READ(11,11)(NTIME(I),TDBAA(I),I=1,M)
                C     TDBAA = TEMPERATURE DRY BULB BEFORE CONVERSION
0030               READ(11,11)(NTIME(I),TDBBA(I),I=1,M)
                C     TDBBA = TEMPERATURE DRY BULB BEFORE CONVERSION ABOVE SURFACE
0031               READ(11,20)(NTIME(I),ROUTA(I),I=1,M)
                C     ROUTA = OUT GOING RADIATION BEFORE CONVERSION
0032               READ(11,20)(NTIME(I),RSOLA(I),I=1,M)
```

```
C     RSOLA = SOLAR RADIATION BEFORE CONVERSION
0033        READ(11,20)(NTIME(I),RFRIA(I),I=1,M)
C     RFRIA = NET RADIATION FRITCHEN BEFORE CONVERSION
0034        READ(11,20)(NTIME(I),SFLXA(I),I=1,M)
C     SFLXA = SOIL HEAT FLUX BEFORE CONVERSION
0035        READ(11,11)(NTIME(I),ZO(I),I=1,M)
C     ZO=ROUGHNESS PARAMETER
0036        READ(11,20)(NTIME(I),DISP(I),I=1,M)
C     DISP = HEIGHT DISPLACEMENT PARAMETER
0037        READ(11,11)(NTIME(I),WSPDBA(I),I=1,M)
C     WSPDBA HAS UNITS MILE/HR,WSPDB IS IN CM/SEC
0038        READ(11,11)(NTIME(I),TSFA(I),I=1,M)
C     TSFA = TEMPERATURE OF PLANT SURFACE USING BARNES RADIOMETER
0039        P=1013.
0040        TS=373.16
0041        DENA=1.2E-3
C     DENA = DENSITY OF AIR IN GM/CME3 = 1.2E-3
0042        SPHT=.242
C     SPHT = SPECIFIC HEAT OF AIR = .242CAL/GM DEGREE C
0043        CPSY=.65
C     CPSY = PSYCHROMETRIC CONSTANT IN MB/DEGREE*C = .65
0044        LA=586.
0045        CP=1013.
C     CP=AIR PRESSURE
0046        WMOL=.614334
C     WMOL=RATIO OF MOLECULAR WT WATER TO MOLECULAR WT AIR
0047        DEAIR=1.168E-3
C     DEAIR=AIR DENSITY=1.168E-3
0048        CVK=.41
C     CVK=VONKARMAN CONSTANT=.4
0049        HTCON=.008
C     HTCON = HEIGHT CONSTANT FOR DIFFERENT HEIGHT CROPS
0050        ZB=80.
C     ZB=ELEVATION ABOVE SURFACE
0051        DO 18 I=1,M
0052        TSF(I)=-1.342296*TSFA(I)-.007999927*TSFA(I)**2+77.37787
C     TSF = TEMPERATURE AT SURFACE DEGREE C BARNES
0053        XTIME(I)=XHOUR(I)*60+XMINT(I)
0054        TDBA(I)=-.627*(2.*TDBAA(I))**2+22.379*2.*TDBAA(I)+65.45
C     TDBA = TEMPERATURE DRY BULB AT SURFACE
0055        TDBB(I)=-.627*(2.*TDBBA(I))**2+22.379*2.*TDBBA(I)+65.45
C     TDBB = TEMPERATURE DRY BULB ABOVE SURFACE
0056        TDPA(I)=(TDPAF(I)-32.)*5./9.
C     TDPA = TEMPERATURE DEW POINT AT SURFACE
0057        TDPB(I)=(TDPBF(I)-32.)*5./9.
C     TDPB = TEMPERATURE DEW POINT ABOVE SURFACE
0058        RSOL(I)=.02*RSOLA(I)/1.98
C     RSOL = SOLAR RADIATION
0059        RLOT(I)=.02*RLOTA(I)/8.57
C     RLOT = OUT GOING RADIATION
0060        ALEB(I)=RLOT(I)/RSOL(I)
C     ALEB = ALBEDO
0061        SFLX(I)=.02*SFLXA(I)/2.20
C     SFLX = SOIL HEAT FLUX
```

```
0062            RFRI(I)=.02*RFRIA(I)/2.71
                C   RFRI = NET RADIATION FROM FRITCHEN
0063            RNET(I)=RSOL(I)-ROUT(I)
                C   RNET = NET RADIATION
0064            TDBAK(I)=273.16+TDBA(I)
0065            TDBBK(I)=273.16+TDBB(I)
0066            TDPAK(I)=273.16+TDPA(I)
0067            TDPBK(I)=273.16+TDPB(I)
0068            TSFKK(I)=TSF(I)+273.16
                C   TSFKK=SURFACE TEMPERATURE DEGREES K
                C   K SUFFIX INDICATES DEGREE KELVIN
0069            EA(I)=EXP((-7.90298)*(TS/TDPAK(I)-1.)
                1+(5.02808)*ALOG10(TS/TDPAK(I))
                2-(1.3816E-7)*(10)**(11.344)*(1.-TDPAK(I)/TS))-1.)
                3+(8.1328E-3)*(10)**(-3.49149)*(TS/TDPAK(I)-1.))-1.)
                4+ALOG10(1013.246))
                5*(2.302585))
                C.  EA = VAPOR PRESSURE AT SURFACE
0070            EB(I)=EXP((-7.90298)*(TS/TDPBK(I)-1.)
                1+(5.02808)*ALOG10(TS/TDPBK(I))
                2-(1.3816E-7)*(10)**(11.344)*(1.-TDPBK(I)/TS))-1.)
                3+(8.1328E-3)*(10)**(-3.49149)*(TS/TDPBK(I)-1.))-1.)
                4+ALOG10(1013.246))
                5*(2.302585))
                C   EB = VAPOR PRESSURE ABOVE SURFACE
0071            ESA(I)=EXP((-7.90298)*(TS/TDBAK(I)-1.)
                1+(5.02808)*ALOG10(TS/TDBAK(I))
                2-(1.3816E-7)*(10)**(11.344)*(1.-TDBAK(I)/TS))-1.)
                3+(8.1328E-3)*(10)**(-3.49149)*(TS/TDBAK(I)-1.))-1.)
                4+ALOG10(1013.246))
                5*(2.302585))
                C   ESA = SATURATED VAPOR AT SURFACE
0072            ESB(I)=EXP((-7.90298)*(TS/TDBBK(I)-1.)
                1+(5.02808)*ALOG10(TS/TDBBK(I))
                2-(1.3816E-7)*(10)**(11.344)*(1.-TDBBK(I)/TS))-1.)
                3+(8.1328E-3)*(10)**(-3.49149)*(TS/TDBBK(I)-1.))-1.)
                4+ALOG10(1013.246))
                5*(2.302585))
                C   ESB = SATURATED VAPOR PRESSURE ABOVE SURFACE
0073            ESC(I)=EXP((-7.90298)*(TS/TSFKK(I)-1.)
                1+(5.02808)*ALOG10(TS/TSFKK(I))
                2-(1.3816E-7)*(10)**(11.344)*(1.-TSFKK(I)/TS))-1.)
                3+(8.1328E-3)*(10)**(-3.49149)*(TS/TSFKK(I)-1.))-1.)
                4+ALOG10(1013.246))
                5*(2.302585))
                C   ESC=SATURATION VAPOR PRESSURE AT TSF
0074            RHA(I)=EA(I)/ESA(I)*100.
                C   RHA = RELATIVE HUMIDITY AT SURFACE
0075            RHB(I)=EB(I)/ESB(I)*100.
                C   RHB = RELATIVE HUMIDITY ABOVE SURFACE
0076            EVAD(I)=ESB(I)-EB(I)
                C   EVAD=VAPOR PRESSURE DEFICITE
0077            B(I)=.46*((TDBA(I)-TDBB(I))/(EA(I)-EB(I)))*(P/760.)
                C   B = BOWEN RATIO
```

```
0078            TEVT(I)=(TSF(I)+TDBB(I)/2.)
              C     TEVT=(SURFACE TEMP+AIR TEMP AT Z8)/2
0079            WSPDB(I)=WSPDBA(I)*44.704
              C     WSPDB=WIND SPEED AT HEIGHT B
0080            HTP(I)=(DEAIR*(CVK**2)*WSPDB(I))/(ALOG((160-DISP(I))/ZO(I)))**2
              C     HTP = TRANSPORT COEFFICIENT FOR HEAT AND WATER VAPOR
0081            TFC(I)=(DEAIR*AMOL*CVK*WSPDB(I))/(CP*(ALOG(Z8/ZO(I)))**2)
              C     TFC=TRANSFER COEFFICIENT BY VANBAVEL
0082            SEVT(I)=-.03167281+TEVT(I)*.003577485*TEVT(I)**2+1.295031
              C     SEVT=DELTA/GAMMA AT TEMP TEVT
0083            SLOPE(I)=SEVT(I)*CPSY
              C     SLOPE = SLOPE OF SATURATION VAPOR CURVE VERSUS TEMP IN MB/DEGREE C
0084            HENG(I)=RNET(I)+SELX(I)
              C     HENG=SUM OF ENERGY INPUTS FOR VANBAVEL
0085            ETVB(I)=(SEVT(I)*HENG(I)+LA*TFC(I)*EVAD(I))/((SEVT(I)+1.))
              C     ETVB=ET BY VANBAVEL METHOD
0086            ETBA(I)=(RFRI(I)*SELX(I))/(1.+.65*((TDBB(I)-TSF(I))/(ESB(I)-ESC(I)
                1)))
              C     ETBA = ET CALCULATED BY BARTHOLICS METHOD
0087            ET(I)=RFRI(I)-586.*(WMOL*DENA*CVK*HTCON*6.05E-4*(TSF(I)-TDBB(I))
                1/ALOG(CVK*HTCON*Z8/.25))
0088         18 ETRN(I)=(RFRI(I)-SELX(I))/(1.+B(I))
              C     ETRN = ET DETERMINED BY ENERGY BALANCE EQUATION
0089          5 FORMAT(1H ,7(I5,1X,F5.2,2X))
0090          8 FORMAT(1H ,7(I5,1X,F5.2,2X))
0091         16 FORMAT(1H ,7(I5,1X,F5.2,2X))
0092         30 FORMAT(1H ,7(I5,1X,F5.4,2X))
0093         32 FORMAT(1H ,7(I5,1X,F5.2,2X))
0094            WRITE(12,14)NDATE
0095         14 FORMAT(1HO,55HDATA COLLECTED AT REDFIELD ON GRAIN SORGHUM STARTING
                1 ,I5)
0096            WRITE(12,15)
0097         15 FORMAT(1HO,30HVAPOR PRESSURE AT FIRST HEIGHT)
0098            WRITE(12,16)(NTIME(I),EA(I),I=1,M)
0099            WRITE(12,6)
0100          6 FORMAT(1HO,31HVAPOR PRESSURE AT SECOND HEIGHT)
0101            WRITE(12,5)(NTIME(I),EB(I),I=1,M)
0102            WRITE(12,24)
0103         24 FORMAT(1HO,36HSATURATION VAPOR PRESSURE AT SURFACE)
0104            WRITE(12,8)(NTIME(I),ESA(I),I=1,M)
0105            WRITE(12,25)
0106         25 FORMAT(1HO,39HSATURATION VAPOR PRESSURE ABOVE SURFACE)
0107            WRITE(12,8)(NTIME(I),ESB(I),I=1,M)
0108            WRITE(12,33)
0109         33 FORMAT(1HO,26HAIR TEMPERATURE AT SURFACE)
0110            WRITE(12,8)(NTIME(I),TDBA(I),I=1,M)
0111            WRITE(12,29)
0112         29 FORMAT(1HO,38HAIR TEMPERATURE ABOVE SURFACE DEGREE C)
0113            WRITE(12,8)(NTIME(I),TDBB(I),I=1,M)
0114            WRITE(12,34)
0115         34 FORMAT(1HO,51HDEWPOINT TEMPERATURE AT SURFACE)
0116            WRITE(12,8)(NTIME(I),TDPA(I),I=1,M)
0117            WRITE(12,35)
0118         35 FORMAT(1HO,34HDEWPOINT TEMPERATURE ABOVE SURFACE)
```

```
0119              WRITE(12,8)(NTIME(I),TDPB(I),I=1,M)
0120              WRITE(12,7)
0121            7 FORMAT(1HO,33HRELATIVE HUMIDITY AT FIRST HEIGHT)
0122              WRITE(12,8)(NTIME(I),RHA(I),I=1,M)
0123              WRITE(12,9)
0124            9 FORMAT(1HO,34HRELATIVE HUMIDITY AT SECOND HEIGHT)
0125              WRITE(12,8)(NTIME(I),RHB(I),I=1,M)
0126              WRITE(12,31)
0127           31 FORMAT(1HO,21HBOWEN RATIO)
0128              WRITE(12,32)(NTIME(I),B(I),I=1,M)
0129              WRITE(12,27)
0130           27 FORMAT(1HO,24HINCOMING SOLAR RADIATION)
0131              WRITE(12,5)(NTIME(I),RSOL(I),I=1,M)
0132              WRITE(12,21)
0133           21 FORMAT(1HO,6HALBEDO)
0134              WRITE(12,5)(NTIME(I),ALEB(I),I=1,M)
0135              WRITE(12,26)
0136           26 FORMAT(1HO,23HHEAT FLUX INTO THE SOIL)
0137              WRITE(12,8)(NTIME(I),SFLX(I),I=1,M)
0138              WRITE(12,23)
0139           23 FORMAT(1HO,19HET BY ENERGY BUDGET)
0140              WRITE(12,30)(NTIME(I),ETRN(I),I=1,M)
0141              WRITE(12,36)
0142           36 FORMAT(1HO,14HET BY VANBAVEL)
0143              WRITE(12,30)(NTIME(I),ETVB(I),I=1,M)
0144              WRITE(12,37)
0145           37 FORMAT(1HO,15HET BY BARTHOLIC)
0146              WRITE(12,30)(NTIME(I),ETBA(I),I=1,M)
0147           38 FORMAT(1HO,13HET BY CARLSON)
0148              WRITE(12,40)
0149              WRITE(12,8)(NTIME(I),ET(I),I=1,M)
0150              CALL PLOTA(IMAGE,XMIN,XMAX,YMIN,YMAX)
0151              CALL PLOTB(XTIME,ET,4HOOO$,M)
0152              CALL PLOTB(XTIME,ETRN,4HOCO*,M)
0153              CALL PLOTB(XTIME,ETBA,4HOCO&,M)
0154              CALL PLOTB(XTIME,ETVB,4HOCO-,M)
0155              CALL PLOTC(HEAD,18,CRD,12,ABSC,16)
0156              CALL PLOTA(IMAGE,XMIN,XMAX,YMI,YMA)
0157              CALL PLOTB(XTIME,RSOL,4HCCO*,M)
0158              CALL PLOTB(XTIME,RNET,4HOCO&,M)
0159              CALL PLOTB(XTIME,ALEB,4HOCO$,M)
0160              CALL PLOTC(HEADA,19,CRDA,12,ABSC,16)
0161              GO TO 10
0162           50 STOP
0163              END
```

# APPENDIX II

## THERMOPILE PSYCHROMETER

In the collection of data we had difficulties in the determination of accurate vapor pressure data for use in the Bowen Ratio. In an attempt to improve the determination of Bowen Ratio data we have designed a five thermocouple thermopile psychrometer.

The thermopile psychrometer as designed and shown in Figure A.1 is unique in that it measures differences between the wet and dry bulb temperatures of a particular height and the differences of the dry bulb temperatures of a particular height and the difference of the dry bulb temperatures between the two heights. By doing this we measure the values needed for the Bowen Ratio equation rather than the actual values which must be converted into differences.

Potential across AB = dry bulb temperature - wet bulb temperature at level 1.

Potential across CD = dry bulb temperature at level 1.

Potential across DE = dry bulb temperature at level 1 - dry bulb temperature at level 2.

Potential across FG = dry bulb temperature at level 2.

Potential across GH = dry bulb temperature - wet bulb temperature at level 2.

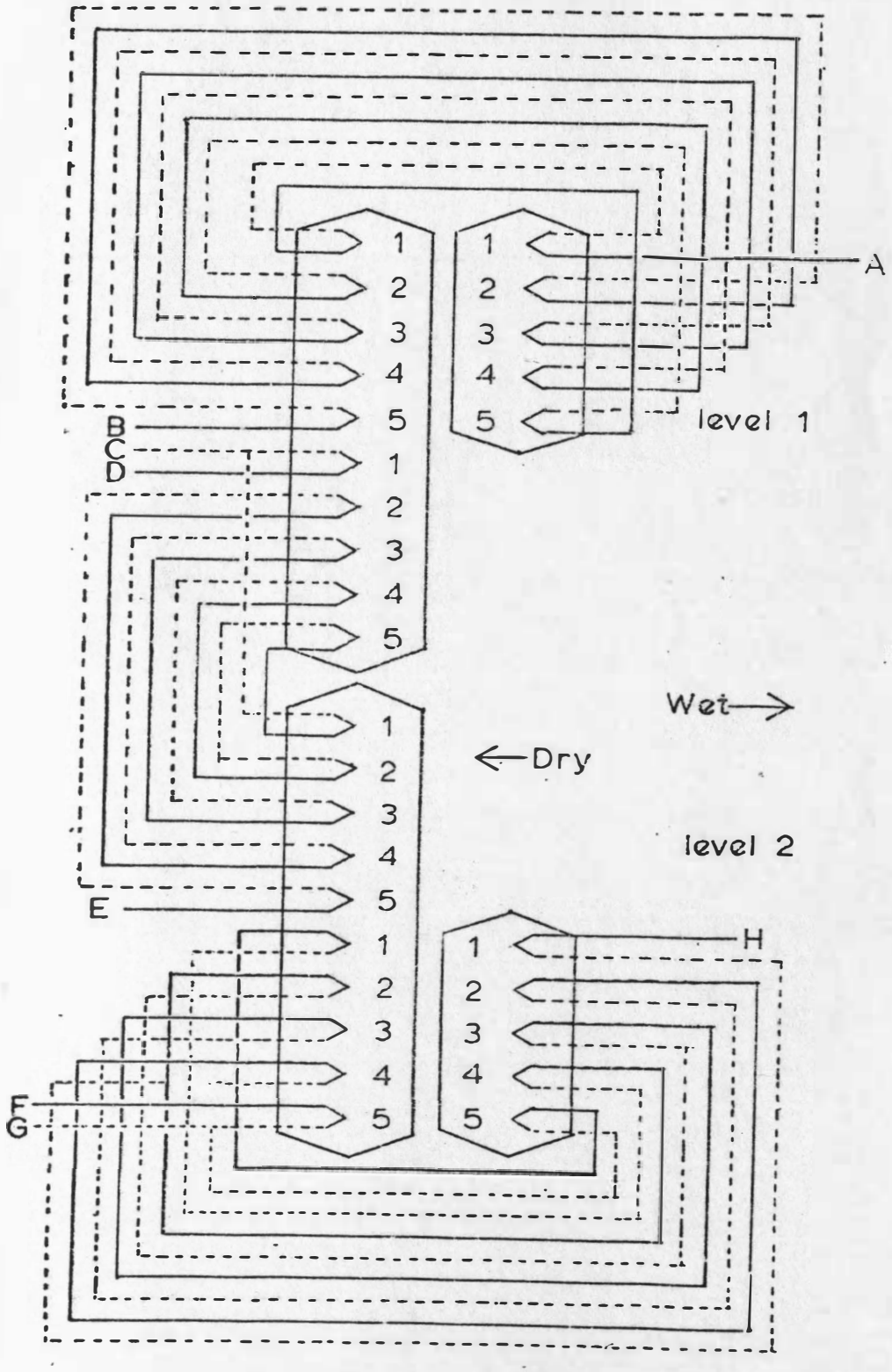


Figure A.1. Wiring diagram of thermocouple psychrometer.